Journal of Medicinal Chemistry

Article

Discovery of Potent, Selective, and Direct Acid Sphingomyelinase Inhibitors with Antidepressant Activity

Kan Yang, Jinying Yu, Keyi Nong, Youzhi Wang, Ao Niu, Wenlu Chen, Jibin Dong, and Jinxin Wang

J. Med. Chem., **Just Accepted Manuscript** • DOI: 10.1021/acs.jmedchem.9b00739 • Publication Date (Web): 16 Jan 2020

Discovery of Potent, Selective, and Direct Acid Sphingomyelinase Inhibitors with Antidepressant Activity

Kan Yang[1,2], Jinying Yu[1], Keyi Nong[1], Youzhi Wang[1], Ao Niu[1], Wenlu Chen[1], Jibin Dong[3], Jinxin Wang[1]**

[1]Jiangsu Key Laboratory of Drug Design and Optimization, Department of Medicinal Chemistry, School of Pharmacy, China Pharmaceutical University, Nanjing 210009, China

[2]Key Laboratory of Pharmaceutical Quality Control of Hebei Province, College of Pharmaceutical Sciences, Hebei University, Baoding 071002, China

[3]Department of Biochemistry, School of Pharmacy, Fudan University, Shanghai 201203, China

Abstract

Recent studies on sphingolipids suggest that acid sphingomyelinase (ASM) which plays a central role in the pathogenesis of major depression, is emerging to be a novel target for developing antidepressants. Herein we firstly described the design, synthesis, and biological evaluation of hydroxamic acid-based direct inhibitors of

ASM with the effort of validating their antidepressant effects *in vivo*. As a result, a series of novel ASM inhibitors were developed using a structure-based approach. Our studies demonstrated that the administration of **21b** improved depression-like behaviors of rats. Importantly, this positive result was relevant to the inhibition of ASM and the increasing neurogenesis in hippocampus. To the best of our knowledge, this is the first time that direct inhibitors of ASM were developed to support the possibility of ASM as a potential therapeutic target for depression.

Introduction

Major depression disorder (MDD) is a severe, chronic and life-threatening illness, which is regarded as a significant cause of global disability and mortality.[1] It usually takes several weeks for the currently used antidepressants to achieve remarkable effectiveness. However, adverse effects of clinical antidepressants occur faster, such as sexual dysfunction, nausea/vomiting, and sleep disruption.[2] Moreover, 12 % – 20 % of MDD patients have developed drug resistance.[3] The mechanism of MDD is complicated.[4] Previously, the lack of monoaminergic neurotransmitters was the focus of pathophysiological concepts. Most antidepressant drugs were found regulating extracellular concentration of serotonin and norepinephrine. However, the activity of some antidepressants did not correlate with their monoaminergic effect. With the growing understanding of the mechanism of depression, the reduction in neurogenesis, particularly in the hippocampus, has been raised as a central factor of

MDD.[5-7] Thus, the recent advances that ASM plays a central role in neurogenesis and may be a noteworthy target for the development of novel anti-depressants has dawn our attention. [8-10]

ASM is a zinc-dependent enzyme that acts as a lysosomal or secretory hydrolase, catalyzing the degradation of sphingomyelin (SM) to phosphorylcholine and ceramide (Cers). The released Cers molecules in the cell membrane or mitochondrial membrane can spontaneously form Cers-enriched "lipid platforms",[11] which serve to trap and cluster receptor molecules and to initiate stress and apoptotic signals. Additionally, Cers can directly regulating a series of apoptotic signals, such as protein kinase C isoforms [12] and cathepsin D.[13] Thus, Cers have been regarded as pivotal factors in the regulation of apoptosis.[14-16]

Clinical studies demonstrated that depressed patients displayed significantly higher levels of ASM activity and Cers concentration in their cultivated blood cells or plasma compared to the control groups.[17, 18] Furthermore, splicing events of ASM were found less occurring in MDD patients, which led to higher expression of ASM.[19] Another direct and convincing evidence is that most of the antidepressants are functional inhibitors of ASM, which detaches ASM from the inner lysosomal membranes. This will result in the proteolytic degradation of ASM.[20, 21] In 2013, a study from Gulbins's group [22] revealed that the effects of antidepressant drugs might be mediated by the ASM-Cers system through a mechanism of Cers negatively related neuronal

proliferation, maturation, and survival. Administration of amitriptyline and fluoxetine with the therapeutic concentrations not only reduced hippocampus ASM activity and Cers concentrations, but also increased hippocampus neurogenesis. [22] In addition, it was found that the inhibition of ASM could prevent the stress-induced P38 activation, thereby increasing neurogenesis and reducing depression-like symptoms.[23] A recent study revealed that free-choice alcohol drinking reduced depression-like behavior in depressed animals through the normalization of brain ASM activity.[24] All together, these studies demonstrated that ASM is a promising drug target to develop new antidepressant agents (Figure 1).

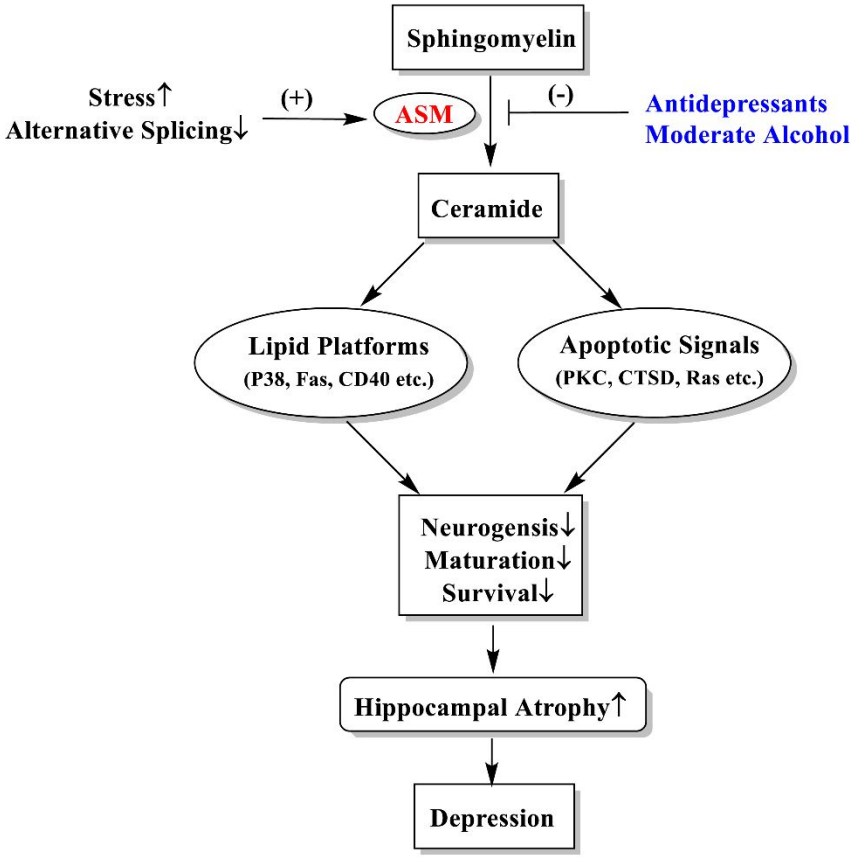

Figure 1 Supposed mechanism of acid sphingomyelinase in the development of depression. ASM, acid sphingomyelinase

Inhibition of ASM could promote neurogenesis and reduce depression-like behavior. However, until now, direct inhibitors of ASM are few,[25] including analogues of SM,[26] bisphosphonates,[27] phosphatidylinositol-3,5-bisphosphates derivatives,[28, 29] benzopyrone derivatives,[30] and xanthones (Figure 2).[31, 32] Therefore, in this work, we developed novel direct inhibitors of ASM to disclose the role of ASM in MDD and to verify the effectiveness of ASM as an anti-depression target.

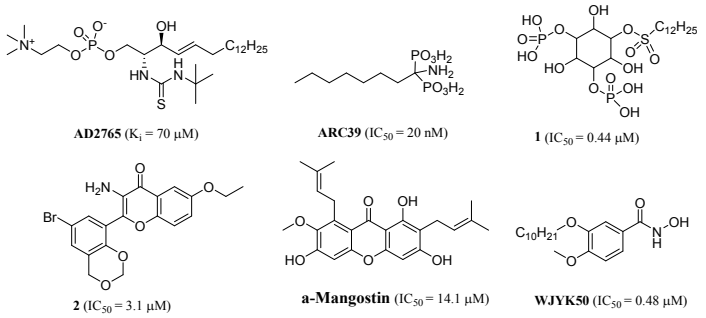

Figure 2 Representative structures of acid sphingomyelinase inhibitors.

Previously, our research group have identified a family of direct ASM inhibitors using a ligand-based pharmacophore model and confirmed a hydroxamic acid group as an essential Zn^{2+} bonding group (ZBG), which led to the discovery of **WJYK50** (IC_{50} = 0.48 μM, Figure 2).[33] In our previous pharmacokinetics study, **WJYK50** showed some deficiencies In this work, a structure-based design approach was performed for the first time to discover novel hydroxamic acid-based ASM direct inhibitors. As a result, a series of new compounds were identified as effective and

selective ASM inhibitors, among which compound **21b** was assessed with *in vivo* behavioral tests, enzyme inhibitory activity test, and neurogenesis studies. Collectively, the promising and innovative results obtained from this study further validated the possibility of targeting ASM to prevent and treat major depression.

Results and discussion

Design of novel ASM inhibitors

In 2016, three research groups resolved the crystal structures of ASM.[34-36] These breakthroughs revealed a large ligand binding cavity defined by certain residues in ASM protein and provided possibilities for structure-based drug design. Firstly, molecular docking simulation was carried out to gain insight into the detail binding mode of **WJYK50** in ASM (PDB code: 5fi9). The hydroxamic acid group of **WJYK50** inserted into the di-zinc catalytic center, whereas its ten-carbon lipid tail sat in a relatively featureless shallow groove in a linear mode (Figure 3A). This binding conformation was very similar to that of the known inhibitor **ARC39**. Both the alkyl chain of **ARC39** and **WJYK50** did not locate to the position of SM fatty-acid chains, which sat along a hydrophobic track that extended from the edge of the active site to the saposin domain.[34] The polar hydroxamic acid head of **WJYK50** competitively occupied the catalytic site where the choline headgroup of SM located to. Moreover, this group made hydrogen bond contacts with residues His208, Asp276 and His280. His280 has been regarded as the key residue for protonation of the ester oxygen of

substrate SM (Figure 3B).[35] Reducing the flexibility of **WJYK50** by replacing flexible alkyl chain with rigid rings might improve π-π or p-π interactions with ASM. Thus, the single benzene of **WJYK50** was replaced by a (benzyloxy)benzene scaffold (Figure 3C). Substitutions of the two benzene rings were also explored. This led to the design of compounds **9a** – **9i** and **12a** – **12j** (Table 1 and Table 2).

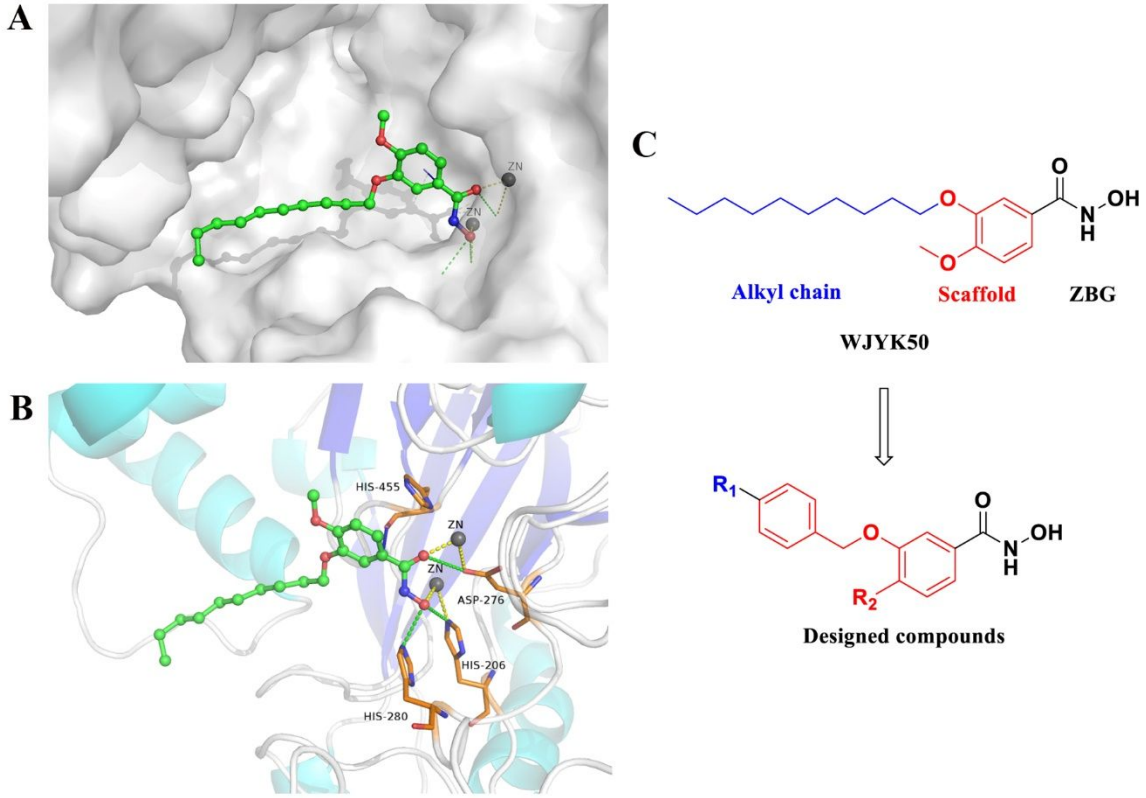

Figure 3 Docking pose of **WJYK50** in acid sphingomyelinase and optimizing strategy. Hydrogen bonds are shown as green lines and metal contacts in yellow.

Enzyme inhibitory activity screening and structure–activity relationship studies of compounds 9a – 9i and 12a – 12j.

Enzymatic assays of the target compounds against ASM and neutral sphingomyelinase (NSM) were performed by evaluating their abilities of inhibiting the production of 7-nitro-2-1,3-benzoxadiazol (NBD)-labeled ceramide. Results were shown in Table 1 and Table 2. These compounds varied with the type and size of substituent group on the ring B as well as the R_2 group at C-4 position of ring A. Overall, most compounds with a biphenyl scaffold showed low micromole IC_{50} values, among which compound **9f** was found to be the most active compound. In addition, the fact that compound **9f** was far more potent than **9g** identified the chlorine substituent on the terminal benzene as a key element for ASM inhibition. Same phenomenon was observed between **9c** and **9b**. Replacement of the terminal benzene by pyridine (**9d** and **9h**) led to great decrease of inhibitory potency. The introduction of C_6H_{13} alkyl also resulted in low micromole ASM inhibition, like **9e**. Compounds **12b – 12e** and **12j** almost lost potency. However, compound **12f** and **12g** were more active than **12a – 12e.** Because of the presence of methylene in R_1 group, **12f** and **12g** showed a little more flexibility than **12b – 12e**. This result indicated that the direct connection of three aromatic rings was unfavorable for their inhibitory activity against ASM, which implied that these structures shouldn't be strongly rigid. Furthermore, bulky substitutes were not suitable for ring B due to the weak activity of **9a** – **9h** when comparing with **9i** and **12a** – **12j**. Furthermore, these active compounds were tested their activity against neutral sphingomyelinase (NSM) to

demonstrate their selectivity. As a result, none of these compounds inhibited NSM at a concentration of 100 μM.

Table 1. Structures of **9a** – **9i** and their inhibitory activity against ASM and NSM.

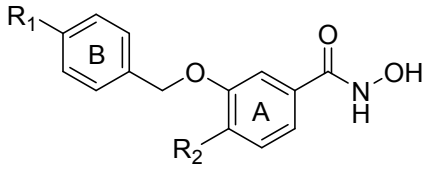

Compound	R_1	R_2	IC_{50} (μM)	
			ASM [a]	NSM [b]
9a	C_6H_{13}	H	2.11 ± 0.30	- [c]
9b	Phenyl	H	19.61 ± 2.98	-
9c	4-Cl-Phenyl	H	8.96 ± 2.03	nt [d]
9d	Pyridin-3-yl	H	52.3 ± 4.98	nt
9e	C_6H_{13}	OMe	1.96 ± 0.23	-
9f	4-Cl-Phenyl	OMe	0.34 ± 0.05	-
9g	Phenyl	OMe	3.63 ± 0.34	-
9h	Pyridin-3-yl	OMe	4.97 ± 1.01	-
9i	Styryl	H	>100	nt
WJYK50			0.48 ± 0.10	nt

[a]ASM, acid sphingomyelinase. [b]NSM, neutral sphingomyelinase. [c]-, inactive at 100 μM. [d]nt, not tested. Data are expressed as means ± SD of 3 experiments.

Table 2. Structures of **12a** – **12j** and their inhibitory activity against ASM and NSM.

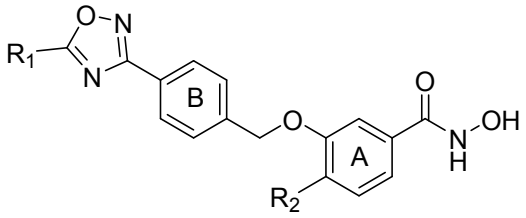

Compound	R_1	R_2	IC_{50} (μM)	
			ASM [a]	NSM [b]
12a	Ethyl	H	34.72 ± 3.25	nt [c]
12b	Phenyl	H	>100	nt
12c	4-Br-Phenyl	H	>100	nt
12d	2-F-Phenyl	H	>100	nt
12e	3-F-Phenyl	H	>100	nt
12f	Benzyl	H	7.83 ± 1.90	nt
12g	Phenethyl	H	1.73 ± 0.20	- [d]
12h	Ethyl	OMe	8.22 ± 1.30	nt

12i	Phenyl	OMe	15.91 ± 1.32	nt
12j	4-Br-Phenyl	OMe	>100	nt

[a]ASM, acid sphingomyelinase. [b]NSM, neutral sphingomyelinase. [c]nt, not tested. [d]-, inactive at 100 μM. Data are expressed as means ± SD of 3 experiments.

Design of compounds 15a – 15e, 18, and 21a – 21b

Most of the compounds were quite hydrophobic and insoluble in physiological saline due to their three benzene rings, such as **9a – 9c**, **9e – 9g**. Thus, we decided to replace ring A or ring B by a heterocyclic ring, which might improve the drug likeness. Moreover, it was found that the imidazole of His457 lies under the ring A of **9f** by docking **9f** into ASM (Figure 4). Therefore, if ring A was optimized to a smaller heterocycle to make the molecular going deep into the catalytic pocket, the compounds might form Pi interactions with His457. These facts led to the design of compounds **15a – 15e**, **18**, and **21a – 21b**.

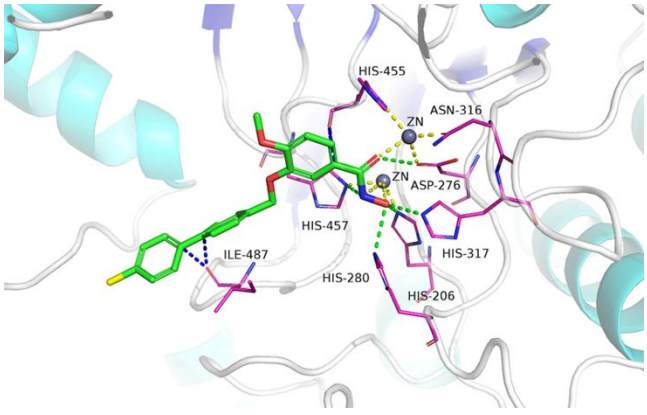

Figure 4 Docking poses of **9f** identified in acid sphingomyelinase. Hydrogen bonds are shown as green lines, metal contacts in yellow, and Pi contacts in blue.

Enzyme inhibitory activity screening and structure–activity relationship studies of 15a –15e, 18, and 21a – 21b

Compound **15a – 15e** showed decreased inhibitory activity on ASM when comparing with **9f** and **9g**, which indicated that hydrophobic benzene was more beneficial than heterocycle at the position of ring B. In accordance with **9f**, attempts to substitute **15a** with a chlorine moiety at either the C-3 (**15c**) or C-4 (**15d**) on the biphenyl ring induced higher potency than **15a**. Placement of a fluorine at C-2 didn't affect the potency because of the similar IC_{50} values of **15a** and **15b.** When ring A was changed to isoxazole, compounds showed comparable activity to **9g** and **9f**. The biphenyl group without any substituent (**21a**) produced moderate ASM inhibition. Compounds **18** and **21b** exhibited higher potency than **21a**. Screening of active compounds against NSM found that all the compounds did not inhibit NSM at 100 μM. Finally, compound **21b** was chosen for further studies.

Table 3. Structures of **15a – 15e** and their inhibitory activity against ASM and NSM.

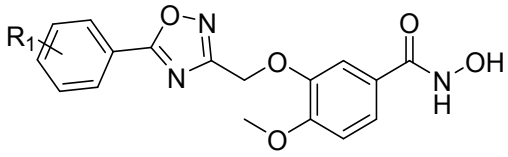

Compound	R_1	IC_{50} (μM)	
		ASM [a]	NSM [b]
15a	H	36.45 ± 1.69	nt [c]
15b	2-F	21.60 ± 1.55	nt
15c	3-Cl	9.22 ± 0.36	- [d]
15d	4-Cl	21.61 ± 2.13	-
15e	3,4- dimethoxy	13.78 ± 0.89	nt

[a]ASM, acid sphingomyelinase. [b]NSM, neutral sphingomyelinase. [c]nt, not tested. [d]-, inactive at 100 μM. Data are expressed as means ± SD of 3 experiments.

Table 4. Structures of **18**, **21a**, **21b** and their inhibitory activity against ASM and NSM.

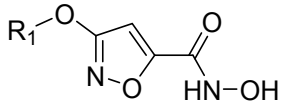

Compound	R_1	IC_{50} (μM)	
		ASM [a]	NSM [b]
18	$C_{10}H_{21}$	0.36 ± 0.06	- [c]
21a	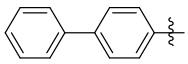	0.88 ± 0.10	-
21b	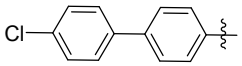	0.32 ± 0.03	-

[a]ASM, acid sphingomyelinase. [b]NSM, neutral sphingomyelinase. [c]-, inactive at 100 μM. [d]nt, not tested. Data are expressed as means ± SD of 3 experiments.

Membrane penetration and brain exposure

Before *in vivo* anti-depressant test, we evaluated the membrane penetration and brain exposure of compound **21b**. Human microvascular endothelial hCMEC/D3 cells were used for membrane transmittance study. As shown in Figure 5, the uptake of **21b** by hCMEC/D3 cells gradually increased from 0.5 h to 2 h, suggesting that **21b** effectively penetrated the cell membrane. However, the uptake of **21b** was decreased at 4 h. This was probably because that cell proliferation led to decreased drug intake at per unit protein. Another possibility was that the cells expelled the drug. By calculating the ratio of the intracellular concentration to the original dose concentration, it was found that the uptake rate of **21b** gradually increased over time, further proving **21b** could successfully penetrate through the cell membrane.

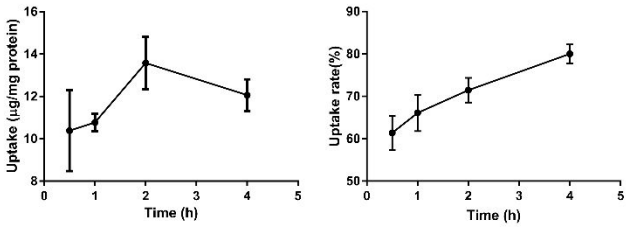

Figure 5 Cellular uptake of **21b** in hCMEC/D3 cells. Values are expressed as mean ± SD from 3 independent experiments.

Then, *in vivo* brain exposure was studied. SD rats were administrated with **21b** at an intraperitoneal dose of 48 mg/kg. Concentrations of **21b** in plasma and brain were quantified by LC-MS/MS. From table 5, it could be found that the drug content in brain tissue was much higher than that in plasma, and this trend was more obvious

over time. This result strongly proved that **21b** penetrated the BBB very well. Besides, the concentrations in brain and plasma were all obviously decreased at 4 h, most probably due to the metabolism.

Table 5. Plasma and brain concentration of **21b** in SD rats.

Time point	Brain Conc. ($ng \cdot g^{-1}$)	Plasma Conc. ($ng \cdot mL^{-1}$)	Brain/Plasma Conc. ratio
0.5 h	2122	709	2.94
2 h	4756	762	6.49
4 h	1298	144	9.55

Values are expressed as mean from 3 independent experiments.

In Vivo Behavioral Studies

Cytotoxicity evaluation using the MTT method supported that **21b** was safe to NIH3T3 cells (IC_{50} =161 ± 33.46 μM) (Figure S4). A functional inhibitor amitriptyline was chosen as positive control and did not showed any cytotoxicity.

Reserpine (4 mg/Kg) was used to induce depression of rats by intraperitoneal injection (ip) daily. Rats were administered compounds **21b** (6, 12, and 24 mg/Kg, ip) or amitriptyline (12 mg/Kg, ip), a tricyclic antidepressant, as well as a functional inhibitor of ASM. Results from sugar water preference test proved that **21b** improved sugar consumption in a dose dependent manner after two days tap-water drinking and following 20 h water depletion and fasting (Figure 6A). In the open-field test, the total time in center of rats were decreased (Figure 6B) and times passing the grid (Figure 4C), frequency of upright (Figure 6D), and frequency of grooming (Figure 6E) were all increased by treating the depressed rats with amitriptyline and **21b**, respectively. In both experiments, the high dose of **21b** showed comparable effects to that of amitriptyline, supporting the notion that inhibiting ASM will generate beneficial effect on depression.

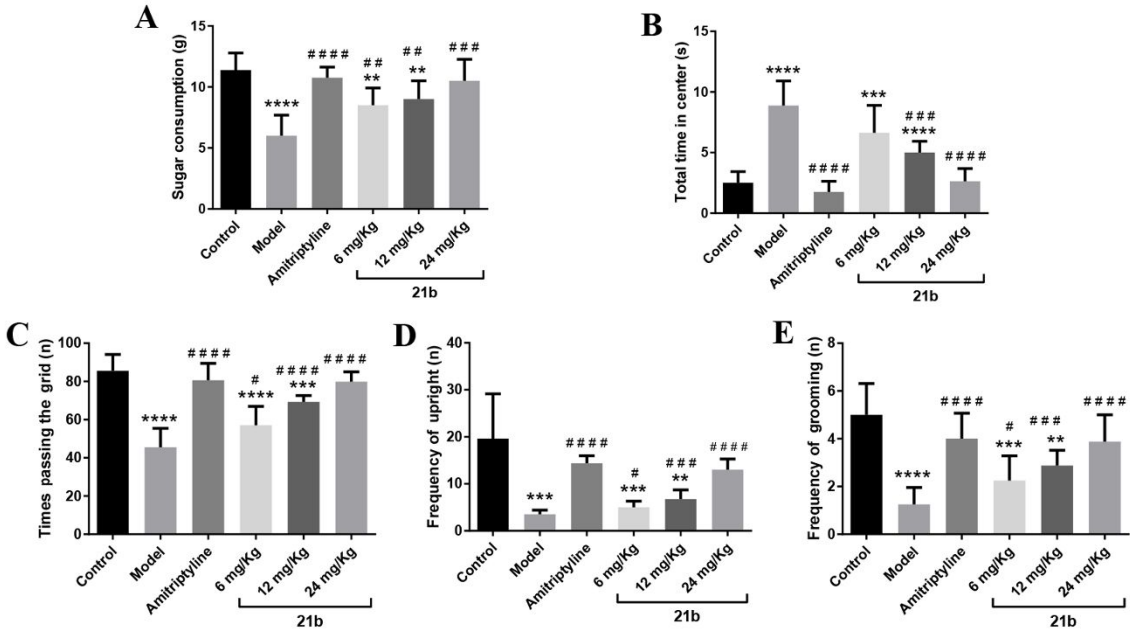

Figure 6 Anti-depressant effect of compound **21b**. Amitriptyline was used as 12 mg/Kg. A, sugar water preference test. B-D, open-field test. Values are expressed as mean ± SD from 8 independent experiments. *, P value compared to control group (**p<0.01, ***p<0.001, ****p<0.0001). #, P value compared the model group (# p<0.05, # # p<0.01, # # # p<0.001, # # # # p<0.0001).

In vivo ASM activity and neurogenesis

To test whether **21b** inhibited ASM in the brain of rats, we separated the cerebral cortex and hippocampus and tested the relative enzyme activity of ASM. As a result, in both the cortex and hippocampus, activity of ASM was obvious increased without treatment of drugs (about 53 % and 73 %, respectively), while this increase in hippocampus was higher than in cortex (Figure 7). Rats administered with **21b** at a dose of 24 mg/Kg demonstrated a reduction of the cortical and hippocampal ASM activity by approximately 27 % and 33 % respectively, comparing to the model group.

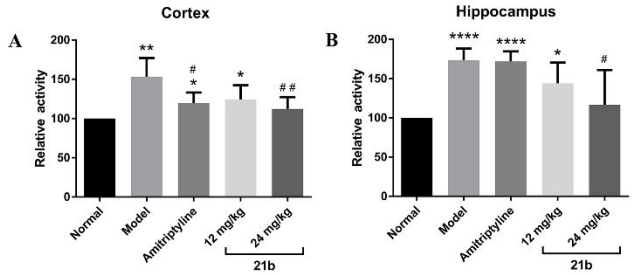

Figure 7 Relative acid sphingomyelinase activity in cerebral cortex and hippocampus. Amitriptyline was used as 12 mg/Kg. The activity of the normal group was regarded as

100 %, and the Y-axis reflected the relative percentage of each group to the normal group. Values are expressed as mean ± SD from 5 independent experiments. *, P value compared to control group (*p<0.05, **p<0.01, ****p<0.0001). #, P value compared the model group (# p<0.05, # # p<0.01).

Meanwhile, to substantiate the role of compound **21b** on neurogenesis, cell proliferation in hippocampus was detected using the EDU method. [37] Treatment of wildtype rats with reserpine resulted in decrease of neurogenesis in the hippocampus (Figure 8), consistent with previously reported data. [22] ASM inhibitor **21b** prevented the inhibitory effect of reserpine on neurogenesis and restored neurogenesis in the brain of depressed rats in a dose dependent manner. Additionally, while amitriptyline exhibited higher anti-depression effect than **21b**, its influence on neurogenesis was less than **21b**. The preferable *in vivo* effects of **21b** was closely consistent with the previous reports on biological studies in the anti-depression potency, ASM activity and neurogenesis. The above findings further confirmed ASM as an effective target for depression treatment.

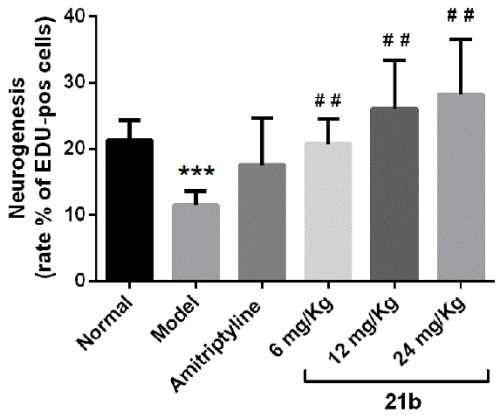

Figure 8 Neurogenesis in hippocampus. The dose of amitriptyline was 12 mg/Kg. Values are expressed as mean ± SD from 5 independent experiments, ***p<0.005 compared to control group, # # p<0.01 compared the model group.

Pure enzyme inhibition of active compounds

We complementally tested the active compounds **9a**, **9c**, **9f**, **9h**, **12f**, **12g**, **18**, **21a**, and **21b** with recombinant human ASM (95% > purity). The results were shown in Table 6. The lead compound, **WJYK50**, showed a slightly higher IC_{50} value (0.89 μM) than the previous one. Compound **9c** (0.36 μM) was found more active than others. And **9f** had an IC_{50} value of 8.07 μM. It was less active than **9c**. This assay led us to ponder that the methoxy group at C-4 position of **WJYK50** should be deleted. Molecule docking strongly indicated that the hydroxamic acid of **9c** binding to ZN702 in a classical bidentate mode (Figure S7). Moreover, the hydroxy and amino groups of hydroxamic acid also combined with the other Zn^{2+} (ZN701) respectively. Compounds

18, **21a**, and **21b** were found unsatisfactory activity in the pure enzyme inhibition assay. As decreased NBD-labeled ceramide generation was detected in the pure enzyme screening assay, our designed compounds can be determined to inhibit ASM in the direct manner.

Table 6. Inhibitory activity against recombinant human ASM.

Compound	Pure ASM [a] (IC_{50}, μM)	Compound	Pure ASM [a] (IC_{50}, μM)

WJYK50	0.89 ± 0.28	**12f**	4.93 ± 1.21
9a	3.38 ±0.37	**12g**	4.25 ± 0.86
9c	0.36 ± 0.11	**18**	2.20 ± 0.36
9f	8.07 ± 0.55	**21a**	4.09 ± 0.48
9h	3.83 ± 0.69	**21b**	3.37 ± 0.82

[a]Pure ASM, recombinant human ASM (purity >95%) was used. Data are expressed as means ± SD of 3 experiments.

Synthesis of the compounds

We began the synthesis from two commercially available materials, **6a** and **6b**. Compounds **6a** or **6b** were substituted by alpha,4-dibromotoluene, yielding compounds **7a** or **7b**, respectively. Compounds **7a** or **7b** were further converted to **8a – 8i** through Heck or Suzuki reactions. The Heck products **8a** and **8b** were reduced to get their corresponding saturated alkyl intermediates. Compounds **6a** or **6b** were respectively substituted by 4-cyanobenyl chloride to yield **10a** or **10b**. **10a** or **10b** were then reacted with hydroxylamine hydrochloride and $NaHCO_3$ in ethanol to yield their amidoximes, which were then respectively reacted with carboxylic acids using EDCI and DMAP to afford 1,2,4-oxadiazole products **11a** – **11j**. In the last step, compounds **8a** – **8i** or **11a** – **11j** were allowed to hydrolyze to give the corresponding carboxylic acids, which were following activated by thionyl chloride and converted

to the hydroxamic acid (**9a** – **9i**) by adding them to a solution of hydroxylamine base. The hydroxylamine solution was freshly prepared from hydroxylamine hydrochloride with NaOH in tetrahydrofuran and water.

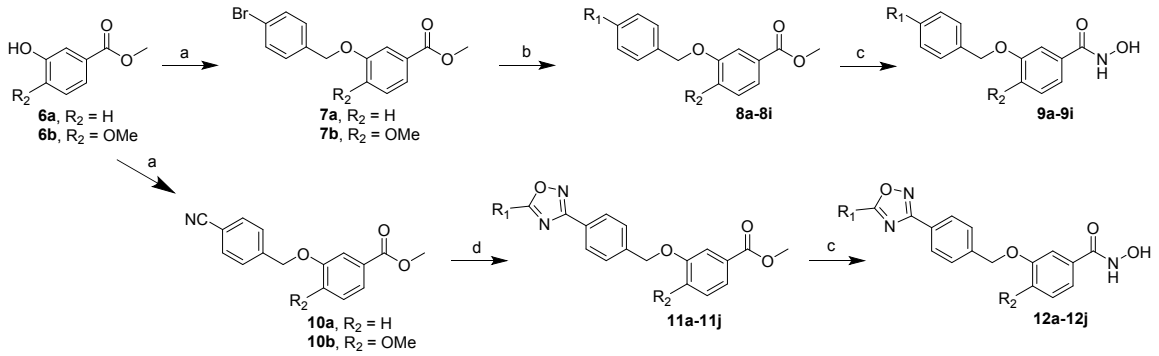

Scheme 1. Reagents and conditions:(a) RBr, K_2CO_3, KI, acetone, 60 °C; (b) Heck: i: 1-Hexene or styrene, Et_3N, $Pd(PPH_3)_2Cl_2$, DMF, 120 °C, or Suzuki: Aromatic boric acid, $CsCO_3$, $Pd(PPh_3)_4$, dioxane, 100 °C; (c) i: NaOH, MeOH, H_2O, 100 °C, ii: $SOCl_2$, DMF, dichloromethane, 40 °C, iii: NaOH, NH_2OH•HCl, THF, H_2O, rt; (d) i: NH_2OH•HCl, $NaHCO_3$, EtOH, 80 °C, ii: Carboxylic acid, EDCI, DMAP, DMF, 0 – 120 °C.

Commercially available material **6b** was substituted by chloroacetonitrile to yield compound **13**. Under the condition of hydroxylamine hydrochloride and $NaHCO_3$ in ethanol, **13** was converted to an active intermediate, which was combined with carboxylic acid and cyclizing at a high temperature to produce compounds **14**. Compound **16** was produced from dimethyl acetylenedicarboxylate and hydroxycarbamide. Compounds **15a – 15e, 17, 29, 20a, 20b** were synthesized

following the same procedure mentioned above. Intermediates **17** or **20** were converted to the title compounds **18** or **21** through a solution of potassium hydroxylamine.

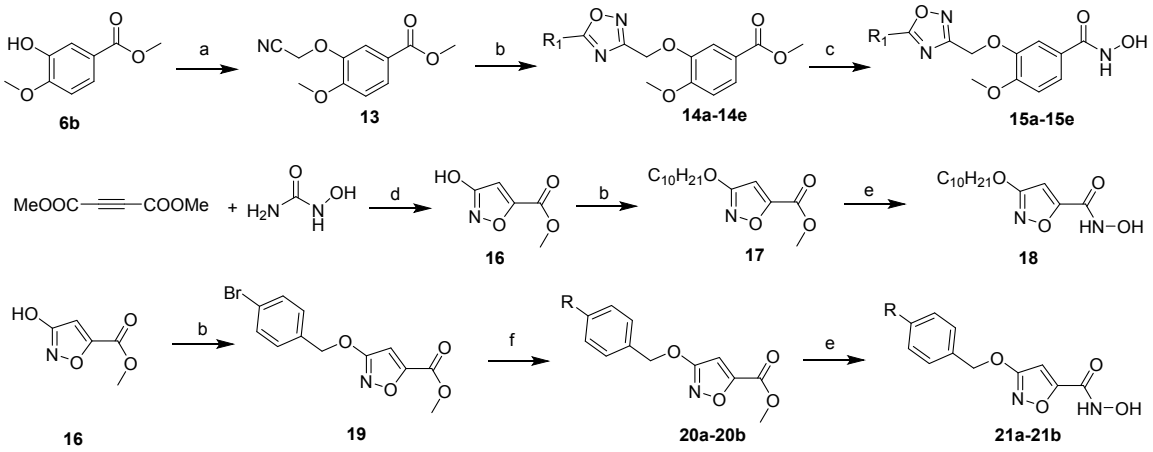

Scheme 2. Reagents and conditions:(a) Chloroacetonitrile, K_2CO_3, KI, acetone, 60 °C; (b) i: NH_2OH•HCl, $NaHCO_3$, EtOH, 80 °C, ii: carboxylic acid, EDCI, DMAP, DMF, 0 – 120 °C; (c) i: NaOH, MeOH, H_2O, 100 °C, ii: $SOCl_2$, DMF, dichloromethane, 40 °C, iii: NaOH, NH_2OH•HCl, THF, H_2O, rt; (d) DBU, MeOH, 0 °C – rt, then 10% HCl; (e) NH_2OK in MeOH, MeOH, rt; (f) Aromatic boric acid, $CsCO_3$, $Pd(PPh_3)_4$, dioxane, 100 °C.

Conclusions

Overall, we disclosed the design, synthesis, and biological screening of a series of direct and selective ASM inhibitors. Through two rounds of optimization, compounds **9a, 9c**, **9f, 9h, 12f, 12g, 18, 21a** and **21b** were identified as effective ASM direct inhibitors. Among those compounds, **21b** showed very low cytotoxicity *in vitro*.

Furthermore, SAR studies reflected that the biphenyl scaffold with a terminal chlorine substituent was necessary for ASM inhibitors. It's worth to note that compound **21b** could permeate the cell membrane well and successfully crossed the blood-brain barrier and distributed in brain tissue. Treatment of depressed rats with **21b** demonstrated favorable antidepressant-like effects in the sugar water preference test and open-field test. Furthermore, this result was in close correlation with the decreased brain ASM activity and restoring neurogenesis in hippocampus by administration of **21b**. Previously, beneficial effects on neurogenesis of the antidepressants have been attributed to their functional inhibition on the ASM/Cers system.[8] In this work, it is the first time to validate the effects on neurogenesis and depression by mean of direct inhibition of ASM.

Altogether, intervention in the ASM/Cers system by small molecule direct inhibitor was applied to provide sufficient evidences in support of ASM as a promising antidepressant target. In addition, this research could offer practical guidance for developing more potent direct ASM inhibitors and serve as a starting point to launch an MDD drug discovery program based this potential target.

Experimental Section

Molecular docking

The docking study was performed with CCDC GOLD 5.3.0 software. The co-crystal structures of ASM with an inhibitor (**ARC39**) (PDB code: 5fi9) was chosen as the

receptor.[33] Small molecules were drawn in ChemDraw and the initial lowest energy conformations were calculated in Chem3D. Protein was preliminary prepared in DS 3.0 with adding hydrogens, deleting glycosyls and water and conducting the "Clean Protein" protocol. The prepared protein was then imported into GOLD and edited with extracting ligand. The binding site was defined at the position of the original included ligand **ARC39**. Goldscore_P450_csd was chosen as the configuration template and GoldScore was chosen as scoring function. Other parameters were kept default. Docking poses were loaded into Gold for a visualization of ligand-receptor interactions and analysis.

Chemistry

General: Starting materials and reagents were obtained from commercially available sources with high–grade purity. Melting points were determined on a MEL-TEMP Ⅱ apparatus (Laboratory Devices, MA, USA). ^{1}H NMR and ^{13}C NMR spectra were recorded on a Bruker AV-300 MHz instrument (Bruker Biospin AG, Switzerland) in $CDCl_3$ or DMSO-d_6 with TMS as the internal standard. MS were obtained on Waters Q-Tof microTM (Waters, MA, USA) with the ESI (+, -) protonation interface. High–resolution mass spectra (HRMS) were recorded on Q-Tof Premier hybrid mass spectrometer with electron spray ionization (ESI). HPLC analysis was performed on a Shimadzu SPD-20A/20AV HPLC system (Shimadzu, Tokyo, Japan). The column used was a C18 column (5 μ micron, 250 × 4.60 mm) at a temperature of 30 °C and a flow

rate of 1.0 mL/min. The purity of title compounds was higher than 95 %, which was assessed at 254 nm using methanol /water (0.1% AcOH) (80:20). All title compounds were examined for PAINS and passed. Anhydrous reactions were carried out in dried glassware under a nitrogen atmosphere. The boiling range for petroleum ether was 60 – 90 °C.

General procedure for the preparation of compounds 7a and 7b.

To a solution of the substrate (**6a** or **6b**, 1 g, 1 equiv.) in acetone was added potassium carbonate (3 equiv.), potassium iodide (0.1 equiv.), and 4-bromobenzyl bromide (1.2 equiv.). The mixture was heated to reflux for 4 h. After the reaction was finished, the mixture was filtered and the filtrate was concentrated and purified by chromatography on silica gel to afford the target products.

General procedure for the preparation of compounds 8a – 8i.

Heck procedure: A mixture of the substrate (**7a** or **7b**, 100 mg, 1 equiv.), alkene (3 equiv.), trans-dichlorobis(triphenyl-phosphine)Palladium(II) (0.05 equiv.), and triethylamine (3 equiv.) in N,N-dimethylformamide (10 mL) was heated to 120 °C for 6 h under N_2 atmosphere. When the reaction was finished, the mixture was diluted with water and extracted by ethyl acetate. The organic phase was washed three times by saline and dried over Na_2SO_4. The solution was concentrated and purified by chromatography on silica gel to afford the target products.

Suzuki procedure: A mixture of the substrate (**7a** or **7b**, 100 mg), aromatic boracic acid (1.5 equiv.), and tetrakis(triphenylphosphine)palladium(0) (0.05 equiv.), and cesium carbonate (2 equiv.) in 1,4-dioxane (10 mL) was heated to 100 ℃ for 4 h under N_2 atmosphere. When the reaction was finished, the mixture was filtered and the solid was washed by dichloromethane. The filtrate was concentrated and purified by chromatography on silica gel to afford the target products.

Methyl (E)-3-((4-(hex-1-en-1-yl)benzyl)oxy)benzoate (8a)

Oil (65 mg, 63.8 %), ^{1}H-NMR (300 MHz, $CDCl_3$): δ 7.70-7.67 (m, 2H), 7.46-7.34 (m, 5H), 7.26-7.17 (m, 2H), 6.44-6.22 (m, 0.5H), 5.59-5.46 (m, 0.5H), 5.13-5.10 (m, 2H), 3.94 (s, 3H), 2.28-2.00 (m, 2H), 1.73-1.28 (m, 4H), 1.02-0.88 (m, 3H); ESI-MS m/z: 325.21 $[M + H]^+$.

Methyl 3-([1,1'-biphenyl]-4-ylmethoxy)benzoate (8b)

White solid (73 mg, 73.0 %), M.P. 84-86 ℃, ^{1}H-NMR (300 MHz, $CDCl_3$): δ 7.68-7.65 (m, 2H), 7.60-7.57 (m, 2H), 7.53-7.51 (m, 4H), 7.43-7.31 (m, 4H), 7.21-7.17 (m, 1H), 5.15 (s, 2H), 3.92 (s, 3H); ESI-MS m/z: 319.1 $[M + H]^+$.

Methyl 3-((4'-chloro-[1,1'-biphenyl]-4-yl)methoxy)benzoate (8c)

White solid (80 mg, 72.3 %), M.P. 118-120 ℃, ^{1}H-NMR (300 MHz, $CDCl_3$): δ 7.70-7.53 (m, 7H), 7.45-7.33 (m, 3H), 7.28 (m, 1H), 7.23-7.20 (m, 1H), 5.17 (s, 2H), 3.94 (s, 3H), 388 (s, 3H); ESI-MS m/z: 375.1 $[M + Na]^+$.

Methyl 3-((4-(pyridin-3-yl)benzyl)oxy)benzoate (8d)

White solid (63 mg, 62.8 %), M.P. 106-107 °C, ^{1}H-NMR (300 MHz, $CDCl_3$): δ 8.86 (m, 1H), 8.61-8.60 (m, 1H), 7.90-7.87 (m, 1H), 7.68-7.55 (m, 6H), 7.40-7.34 (m, 2H), 7.21-7.18 (m, 1H), 5.17 (s, 2H), 3.92 (s, 3H); ESI-MS m/z: 320.1 $[M + H]^+$.

Methyl (E)-3-((4-(hex-1-en-1-yl)benzyl)oxy)-4-methoxybenzoate (8e)

Oil (65 mg, 64.4 %), ^{1}H-NMR (300 MHz, $CDCl_3$): δ 7.70-7.67 (m, 2H), 7.46-7.34 (m, 5H), 7.26-7.17 (m, 2H), 6.44-6.22 (m, 0.5H), 5.59-5.46 (m, 0.5H), 5.13-5.10 (m, 2H), 3.94 (s, 3H), 2.28-2.00 (m, 2H), 1.73-1.28 (m, 4H), 1.02-0.88 (m, 3H); ESI-MS m/z: 325.21 $[M + H]^+$.

Methyl 3-((4'-chloro-[1,1'-biphenyl]-4-yl)methoxy)-4-methoxybenzoate (8f)

White solid (88 mg, 81.2 %), M.P. 140-142 °C, ^{1}H-NMR (300 MHz, $CDCl_3$): δ 7.72-7.68 (m, 1H), 7.64-7.63 (m, 1H), 7.56-7.50 (m, 6H), 7.42-7.39 (m, 2H), 6.93-6.91 (m, 1H), 5.22 (s, 2H), 3.95 (s, 3H), 388 (s, 3H); ESI-MS m/z: 383.1 $[M + H]^+$.

Methyl 3-([1,1'-biphenyl]-4-ylmethoxy)-4-methoxybenzoate (8g)

White solid (78 mg, 78.2 %), M.P. 118-120 °C, ^{1}H-NMR (300 MHz, $CDCl_3$): δ 7.74-7.70 (m, 1H), 7.67-7.55 (m, 7H), 7.49-7.44 (m, 2H), 7.39-7.34 (m, 1H), 6.95-6.93 (m, 1H), 5.24 (s, 2H), 3.97 (s, 3H), 3.90 (s, 3H); ESI-MS m/z: 371.1 $[M + Na]^+$.

Methyl 4-methoxy-3-((4-(pyridin-3-yl)benzyl)oxy)benzoate (8h)

White solid (75 mg, 75.0 %), M.P. 106-107 °C, ^{1}H-NMR (300 MHz, $CDCl_3$): δ 8.87 (m, 1H), 8.62-8.60 (m, 1H), 7.91-7.87 (m, 1H), 7.74-7.70 (m, 2H), 7.65-6.63 (m, 1H),

7.61-7.58 (m, 4H), 7.41-7.36 (m, 1H), 6.96-6.93 (m, 1H), 5.26 (s, 2H), 3.97 (s, 3H), 390 (s, 3H); ESI-MS m/z: 350.2 $[M + H]^+$.

Methyl (E)-3-((4-styrylbenzyl)oxy)benzoate (8i)

Yellow solid (71 mg, 65.6 %), M.P. 137-139 ℃, ^{1}H-NMR (300 MHz, DMSO-d_6): δ 7.68-7.65 (s, 2H), 7.57-7.52 (s, 4H), 7.45-7.43 (m, 2H), 7.40-7.34 (m, 3H), 7.30-7.27 (m, 1H), 7.20(m, 1H), 7.13 (m, 2H), 5.12 (s, 2H), 3.93 (s, 3H); ESI-MS m/z: 345.0 $[M + H]^+$.

General procedure for the preparation of compounds 9a – 9i.

Compounds **8b – 8d, 8f – 8i** (200 mg, 1 equiv.) were respectively hydrolyzed to get the corresponding carboxylic acid under a condition of NaOH (10 equiv.) in methanol and H_2O (v: v = 1:1). Compounds **8a** and **8e** (200 mg, 1 equiv.) were reduced by H_2 in methanol and then hydrolyzed.

A mixture of the hydrolysate (100 mg, 1 equiv.), dimethyl formamide (1 drop) and thionyl chloride (3 equiv.) in anhydrous dichloromethane (10 mL) was heated to reflux for 3 h and concentrated to remove the thionyl chloride and solvent. The concentrate was then re-dissolved by anhydrous tetrahydrofuran (10 mL) and slowly added into a solution of hydroxylamine, which was freshly prepared by dissolving hydroxylammonium chloride (5 equiv.) and NaOH (5 equiv.) into tetrahydrofuran (4 mL) and water (0.5 mL). After the drop add, the mixture was stirred at room

temperature for 5 min, concentrated in vacuum and purified by chromatography on silica gel to afford the title product.

3-((4-Hexylbenzyl)oxy)-N-hydroxybenzamide (9a)

White solid (92 mg, 91.7 %), M.P. 140-141 °C, ^{1}H-NMR (300 MHz, DMSO-d_6): δ 11.21 (s, 1H), 9.06 (s, 1H), 7.37-7.34 (m, 5H), 7.22-7.13 (m, 3H), 5.09 (s, 2H), 2.60 (m, 2H), 1.55 (m, 2H), 1.28 (m, 6H), 0.85 (m, 3H); ^{13}C NMR (75 MHz, DMSO-d_6): δ 164.32, 158.77, 142.56, 134.62, 134.49, 130.01, 128.80, 128.27, 119.71, 118.15, 113.49, 69.74, 35.36, 31.59, 31.42, 28.81, 22.55, 14.42; HRMS (ESI-TOF): calcd for $C_{20}H_{25}NO_3$ $[M + H]^+$ 328.1907, found 328.1913.

3-([1,1'-Biphenyl]-4-ylmethoxy)-N-hydroxybenzamide (9b)

White solid (89 mg, 88.7 %), M.P. 194-196 °C, 1H-NMR (300 MHz, DMSO-d6): δ 11.24 (s, 1H), 9.09 (s, 1H), 7.71-7.36 (m, 12H), 7.20-7.17 (m, 1H), 5.20 (m, 2H); 13C NMR (75 MHz, DMSO-d6): δ 164.29, 158.69, 140.22, 136.51, 134.65, 131.85, 130.07, 129.42, 128.77, 127.99, 127.24, 127.15, 119.77, 118.20, 113.51, 69.45; HRMS (ESI-TOF): calcd for $C_{20}H_{17}NO_3$ [M + H]+ 320.1281, found 320.1285.

3-((4'-Chloro-[1,1'-biphenyl]-4-yl)methoxy)-N-hydroxybenzamide (9c)

White solid (96 mg, 95.7 %), M.P. 165-166 °C, ^{1}H-NMR (300 MHz, DMSO-d_6): δ 11.24 (s, 1H), 9.08 (s, 1H), 7.72-7.69 (m,4H), 7.57-7.51 (m, 4H), 7.43-7.37 (m, 3H), 7.20-7.18 (m, 1H), 5.21 (s, 2H); ^{13}C NMR (75 MHz, DMSO-d_6): δ 164.30, 158.68, 139.04, 138.84, 136.94, 134.67, 132.89, 130.08, 129.37, 128.91, 128.80, 127.21, 119.81,

118.22, 113.55, 69.40; HRMS (ESI-TOF): calcd for $C_{20}H_{16}ClNO_3$ [M + H]$^+$ 354.0891, found 354.0892.

N-hydroxy-3-((4-(pyridin-3-yl)benzyl)oxy)benzamide (9d)

97 White solid (69 mg, 68.7 %), M.P. 172-173 °C, ^{1}H-NMR (300 MHz, DMSO-d_6): δ 11.10 (s, 1H), 8.97 (s, 1H), 8.78 (m, 1H), 8.45 (m, 1H), 7.95 (m, 1H), 7.65-7.06 (m, 9H), 5.09 (s, 2H); ^{13}C NMR (75 MHz, DMSO-d_6): δ 164.18, 158.63, 149.01, 148.11, 137.33, 137.08, 135.67, 134.65, 134.57, 130.08, 128.87, 127.46, 124.37, 119.78, 118.21, 113.49, 69.33; HRMS (ESI-TOF): calcd for $C_{19}H_{16}N_2O_3$ [M + H]$^+$ 302.1387, found 302.1392.

3-((4-Hexylbenzyl)oxy)-N-hydroxy-4-methoxybenzamide (9e)

White solid (79 mg, 78.7 %), M.P. 121-123 °C, 1H-NMR (300 MHz, DMSO-d6): δ 11.08 (s, 1H), 8.94 (s, 1H),7.47-7.45 (m, 1H), 7.40-7.34 (m, 3H), 7.24-7.20 (m, 2H), 7.04-7.01 (m, 1H), 5.05 (s, 2H), 3.80 (s, 3H), 2.61-2.55 (m, 2H), 1.59-1.53 (m, 2H), 1.31-1.24 (m, 6H), 0.88-0.82 (m, 3H); 13C NMR (75 MHz, DMSO-d6): δ 164.37, 151.93, 147.83, 142.62, 134.53, 128.78, 128.64, 128.47, 127.35, 112.28, 111.71, 70.33, 56.08, 35.36, 31.59, 31.44, 28.81, 22.54, 14.43; HRMS (ESI-TOF): calcd for $C_{21}H_{27}NO_4$ [M + H]+ 358.2013, found 358.2018.

3-((4'-Chloro-[1,1'-biphenyl]-4-yl)methoxy)-N-hydroxy-4-methoxybenzamide (9f)

White solid (93 mg, 92.7 %), M.P. 164-165 °C, ^{1}H-NMR (300 MHz, DMSO-d_6): δ 11.08 (s, 1H), 8.93 (s, 1H), 7.74-7.70 (m, 4H), 7.57-7.42 (m, 5H), 7.42-7.39 (m, 1H), 7.06-7.03 (m, 1H), 5.17 (s, 2H), 3.82 (s, 3H); ^{13}C NMR (75 MHz, DMSO-d_6): δ 164.36,

151.96, 147.76, 140.25, 136.55, 131.83, 130.35, 129.44, 128.90, 128.00, 127.23, 127.16, 125.32, 112.31, 111.75, 70.04, 56.13; HRMS (ESI-TOF): calcd for $C_{21}H_{18}ClNO_4$ [M + H]$^+$ 384.0997, found 384.1002.

3-([1,1'-Biphenyl]-4-ylmethoxy)-N-hydroxy-4-methoxybenzamide (9g)

White solid (89 mg, 88.7 %), M.P. 178-179 °C, ^{1}H-NMR (300 MHz, DMSO-d_6): δ 11.11 (s, 1H), 8.95 (s, 1H), 7.69 (m, 4H), 7.57-7.38 (m, 7H), 7.07-7.04 (m, 1H), 5.18 (s, 2H), 3.83(s, 3H); ^{13}C NMR (75 MHz, DMSO-d_6): δ 164.36, 151.98, 147.77, 140.29, 136.57, 129.43, 128.89, 127.99, 127.23, 127.16, 125.34, 120.85, 112.37, 111.78, 70.07, 56.15; HRMS (ESI-TOF): calcd for $C_{21}H_{19}NO_4$ [M + H]$^+$ 350.1387, found 350.1391.

N-hydroxy-4-methoxy-3-((4-(pyridin-3-yl)benzyl)oxy)benzamide (9h)

White solid (70 mg, 69.7 %), M.P. 156-158 °C, 1H-NMR (300 MHz, DMSO-d6): δ 11.11 (s, 1H), 8.92 (m, 2H), 8.58 (m, 1H), 8.11-8.08 (m, 1H), 7.78-7.57 (m, 2H), 7.60-7.40 (m, 5H), 7.06-7.04 (m, 1H), 5.19 (s, 2H), 3.83 (s, 3H); 13C NMR (75 MHz, DMSO-d6): δ 164.34, 151.96, 149.01, 148.11, 147.69, 137.38, 137.09, 135.69, 134.57, 128.96, 127.43, 125.32, 124.36, 120.86, 112.35, 111.78, 69.91, 56.14; HRMS (ESI-TOF): calcd for $C_{20}H_{18}N_2O_4$ [M + H]+ 351.1339, found 351.1341.

(E)-N-hydroxy-3-((4-styrylbenzyl)oxy)benzamide (9i)

White solid (92 mg, 91.7 %), M.P. 188-189 °C, ^{1}H-NMR (300 MHz, DMSO-d_6): δ 11.24 (s, 1H), 9.09 (s, 1H), 7.65-7.60 (m, 4H), 7.48-7.46 (m, 2H), 7.41-7.36 (m, 5H), 7.28 (m, 3H), 7.18-7.16 (m, 1H), 5.16 (s, 2H); ^{13}C NMR (75 MHz, DMSO-d_6): δ 164.30,

158.68, 137.42, 137.16, 136.65, 134.63, 130.06, 129.19, 129.08, 128.60, 128.44, 128.18, 127.02, 126.97, 119.76, 118.20, 113.56, 69.58; HRMS (ESI-TOF): calcd for $C_{22}H_{19}NO_3$ $[M + H]^+$ 364.1438, found 364.1438.

General procedure for the Preparation of compounds 10a and 10b.

To a solution of the substrate (**6a** or **6b**, 1 g, 1 equiv.) in acetone was added potassium carbonate (3 equiv.), potassium iodide (0.1 equiv.), and 4-cyanobenzyl bromide (1.2 equiv.). The mixture was heated to reflux for 4 h. After the reaction was finished, the mixture was filtered and the filtrate was concentrated and purified by chromatography on silica gel to afford the target products.

General procedure for the preparation of compounds 11a – 11j.

Compound **10a** or **10b** (200 mg, 1 equiv.) was added to a mixture of hydroxylamine hydrochloride (5 equiv.) and sodium bicarbonate (7 equiv.) in ethanol. The reaction mixture was heated to 80 °C for 40 min. Upon cooling to room temperature, the reaction was filtered and the filtrate evaporated under reduced pressure. After vacuum drying of the solid in a flask, additional reagents carboxylic acid (1 equiv.), 4-dimethylaminopyridine (0.5 equiv.), and 1-Ethyl-3-(3-dimethylaminopropyl)carbodiimide hydrochloride (2 equiv.) were added into the flask. The mixture was dissolved by N,N-dimethylformamide (2 mL) and stirred for 12 h at room temperature. Then the reaction was heated to 120 °C for 4 h. After the reaction was finished, the mixture was diluted with water and extracted

by ethyl acetate. The organic phase was washed 3 times by saline and dried over Na_2SO_4. The solution was concentrated and purified by chromatography on silica gel to afford the target products.

Methyl 3-((4-(5-ethyl-1,2,4-oxadiazol-3-yl)benzyl)oxy)benzoate (11a)

White solid (142 mg, 56.1 %), M.P. 92-93 °C, ^{1}H-NMR (300 MHz, $CDCl_3$): δ 8.12-8.09 (m, 2H), 7.68-7.65 (m, 2H), 7.57-7.54 (m, 2H), 7.39-7.33 (m, 1H), 7.20-7.16 (m, 1H), 5.17 (s, 2H), 3.92 (s, 3H), 2.98 (q, *J* = 7.62 Hz, 2H), 1.46 (t, *J* = 7.59 Hz, 3H); ESI-MS m/z: 361.1 $[M + Na]^+$.

Methyl 3-((4-(5-phenyl-1,2,4-oxadiazol-3-yl)benzyl)oxy)benzoate (11b)

White solid (174 mg, 60.2 %), M.P.175-176 °C, ^{1}H-NMR (300 MHz, $CDCl_3$): δ 8.26-8.21 (m, 3H), 7.69-7.56 (m, 6H), 7.41-7.36 (m, 2H), 7.23-7.20 (m, 2H), 5.21 (s, 2H), 3.94 (s, 3H); ESI-MS m/z: 409.1 $[M + Na]^+$.

Methyl 3-((4-(5-(4-bromophenyl)-1,2,4-oxadiazol-3-yl)benzyl)oxy)benzoate (11c)

White solid (201 mg, 56.1 %), M.P. 140-141 °C, ^{1}H-NMR (300 MHz, $CDCl_3$): δ 8.22-8.19 (m, 2H), 8.12-8.09 (m, 2H), 7.74-7.68 (m, 4H), 7.62-7.60 (m, 2H), 7.41-7.36 (m, 1H), 7.22-7.20 (m, 1H), 5.21 (s, 2H), 3.94 (s, 3H); ESI-MS m/z: 465.0 $[M + H]^+$.

Methyl 3-((4-(5-(2-fluorophenyl)-1,2,4-oxadiazol-3-yl)benzyl)oxy)benzoate (11d)

White solid (187 mg, 61.8 %), M.P. 123-124 °C, ^{1}H-NMR (300 MHz, $CDCl_3$): δ 8.29-8.23 (m, 2H), 7.71-7.61 (m, 6H), 7.43-7.33 (m, 3H), 6.41-6.32 (m, 6H), 7.24-7.21 (m, 1H), 5.23 (s, 2H), 3.95 (s, 3H); ESI-MS m/z: 405.1 $[M + H]^+$.

Methyl 3-((4-(5-(3-fluorophenyl)-1,2,4-oxadiazol-3-yl)benzyl)oxy)benzoate (11e)

White solid (190 mg, 62.8 %), M.P. 149-150 °C, ^{1}H-NMR (300 MHz, $CDCl_3$): δ 8.23-8.20 (m, 2H), 8.05-8.03 (m, 1H), 7.96-7.93 (m, 1H), 7.70-7.53 (m, 5H), 7.41-7.31 (m, 2H), 7.23-7.19 (m, 1H), 5.21 (s, 2H), 3.94 (s, 3H); ESI-MS m/z: 427.1 $[M + Na]^+$.

Methyl 3-((4-(5-benzyl-1,2,4-oxadiazol-3-yl)benzyl)oxy)benzoate (11f)

White solid (192 mg, 64.1 %), M.P. 86-87 °C, ^{1}H-NMR (300 MHz, $CDCl_3$): δ 8.12-8.10 (m, 2H), 7.69-7.66 (m, 2H), 7.58-7.55 (m, 2H), 6.41-6.32 (m, 6H), 7.21-7.17 (m, 1H), 5.18 (s, 2H), 4.32 (s, 2H), 3.93 (s, 3H); ESI-MS m/z: 401.2 $[M + H]^+$.

Methyl 3-((4-(5-phenethyl-1,2,4-oxadiazol-3-yl)benzyl)oxy)benzoate (11g)

White solid (205 mg, 66.1 %), M.P. 70-72 °C, ^{1}H-NMR (300 MHz, $CDCl_3$): δ 8.13-8.11 (m, 2H), 7.70-7.67 (m, 2H), 7.59-7.57 (m, 2H), 7.41-7.31 (m, 3H), 7.28-7.27 (m, 3H), 7.22-7.18 (m, 1H), 5.19 (s, 2H), 3.93 (s, 3H), 3.32-3.19 (m, 4H); ESI-MS m/z: 415.2 $[M + H]^+$.

Methyl 3-((4-(5-ethyl-1,2,4-oxadiazol-3-yl)benzyl)oxy)-4-methoxybenzoate (11h)

White solid (147 mg, 67.4 %), M.P. 96-97 °C, ^{1}H-NMR (300 MHz, $CDCl_3$): δ 8.10-8.08 (m, 2H), 7.72-7.69 (m, 1H), 7.59-7.57 (m, 3H), 6.94-691 (m, 1H), 5.24 (s, 2H), 3.95 (s, 3H), 3.87 (s, 3H), 2.98 (q, J = 7.62 Hz, 2H), 1.45 (t, J = 7.59 Hz, 3H); ESI-MS m/z: 369.2 $[M + H]^+$.

Methyl 4-methoxy-3-((4-(5-phenyl-1,2,4-oxadiazol-3-yl)benzyl)oxy)benzoate (11i)

White solid (196 mg, 70.1 %), M.P. 159-160 °C, ^{1}H-NMR (300 MHz, $CDCl_3$): δ 8.27-8.21 (m, 4H), 7.75-7.72 (m, 1H), 7.66-7.59 (m, 6H), 6.97-6.94 (m, 1H), 5.29 (s, 2H), 3.99 (s, 3H), 3.90 (s, 3H); ESI-MS m/z: 417.1 $[M + H]^+$.

Methyl

3-((4-(5-(4-bromophenyl)-1,2,4-oxadiazol-3-yl)benzyl)oxy)-4-methoxybenzoate (11j)

White solid (232 mg, 69.8 %), M.P. 156-158 °C, ^{1}H-NMR (300 MHz, $CDCl_3$): δ 8.20-8.17 (m, 2H), 8.11-8.08 (m, 2H), 7.73-7.70 (m, 3H), 7.63-7.61 (m, 3H), 7.41-7.36 (m, 1H), 6.95-6.92 (m, 1H), 5.26 (s, 2H), 3.96 (s, 3H), 3.88 (s, 3H); ESI-MS m/z: 517.0 $[M + Na]^+$.

General procedure for the preparation of compounds 12a – 12j.

Compounds **11a – 11j** were respectively hydrolyzed to get their corresponding carboxylic acid under a condition of NaOH (10 equiv.) in methanol and H_2O (v: v = 1:1). A mixture of the carboxylic acid (100 mg, 1 equiv.), dimethyl formamide (1 drop) and thionyl chloride (3 equiv.) in anhydrous dichloromethane (10 mL) was heated to reflux for 3 h and concentrated to remove the thionyl chloride and solvent. The concentrate was then re-dissolved by anhydrous tetrahydrofuran (10 mL) and slowly added into a solution of hydroxylamine, which was freshly prepared by dissolving hydroxylammonium chloride (5 equiv.) and NaOH (5 equiv.) into tetrahydrofuran (4 mL) and water (0.5 mL). After the drop add, the mixture was

stirred at room temperature for 5 min, concentrated in vacuum and purified by chromatography on silica gel to afford the title product.

3-((4-(5-Ethyl-1,2,4-oxadiazol-3-yl)benzyl)oxy)-N-hydroxybenzamide (12a)

White solid (89 mg, 88.7 %), M.P. 150-151 °C, ^{1}H-NMR (300 MHz, DMSO-d_6): δ 11.21 (s, 1H), 9.05 (s, 1H), 8.05-8.02 (m, 2H), 7.65-7.62 (m, 2H), 7.41-7.34 (m, 3H), 7.19-7.17 (m, 1H), 5.24 (s, 2H), 3.01 (q, J = 6.0 Hz, 2H), 1.34 (t, J = 6.0 Hz, 3H); ^{13}C NMR (75 MHz, DMSO-d_6): δ 181.74, 167.73, 164.26, 158.56, 140.85, 134.68, 130.11, 128.63, 127.60, 126.26, 119.91, 118.20, 113.58, 69.26, 20.07, 10.93; HRMS (ESI-TOF): calcd for $C_{18}H_{17}N_3O_4$ $[M + H]^+$ 340.1292, found 340.1296.

N-hydroxy-3-((4-(5-phenyl-1,2,4-oxadiazol-3-yl)benzyl)oxy)benzamide (12b)

White solid (91 mg, 90.7 %), M.P. 198-199 °C, ^{1}H-NMR (300 MHz, DMSO-d_6): δ 11.25 (s, 1H), 9.10 (s, 1H), 8.21-8.12 (m, 4H), 7.75-7.65 (m, 5H), 7.44-7.38 (m, 3H), 7.21-7.19 (m, 4H), 5.27 (s, 2H); ^{13}C NMR (75 MHz, DMSO-d_6): δ 175.90, 168.51, 164.26, 158.55, 141.11, 134.69, 133.85, 130.11, 130.05, 128.64, 128.40, 127.75, 126.04, 123.80, 119.92, 118.19, 113.61, 69.26; HRMS (ESI-TOF): calcd for $C_{22}H_{17}N_3O_4$ $[M + H]^+$ 388.1292, found 388.1294.

3-((4-(5-(4-Bromophenyl)-1,2,4-oxadiazol-3-yl)benzyl)oxy)-N-hydroxybenzamide (12c)

White solid (93 mg, 92.7 %), M.P. 200-201 °C, ^{1}H-NMR (300 MHz, DMSO-d_6): δ 11.22 (s, 1H), 9.09 (s, 1H), 8.10 (m, 4H), 7.87 (m, 2H), 7.68 (m, 2H), 7.42-7.37 (m, 3H),

7.20 (m, 1H), 5.26 (s, 2H); ^{13}C NMR (75 MHz, DMSO-d_6): δ 175.19, 168.56, 164.21, 158.54, 141.18, 134.68, 133.15, 130.28, 130.11, 128.63, 127.75, 125.87, 122.98, 119.92, 118.18, 113.58, 69.24; HRMS (ESI-TOF): calcd for $C_{22}H_{16}BrN_3O_4$ $[M + H]^+$ 466.0397, found 466.0392.

3-((4-(5-(2-Fluorophenyl)-1,2,4-oxadiazol-3-yl)benzyl)oxy)-N-hydroxybenzamide (12d)

White solid (89 mg, 88.7 %), M.P. 180-181 °C, ^{1}H-NMR (300 MHz, DMSO-d_6): δ 11.19 (s, 1H), 9.02 (s, 1H), 8.25-8.21 (m, 1H), 8.14-8.09 (m, 2H), 7.88-7.076 (m, 1H), 7.70-7.67 (m, 2H), 7.58-7.47 (m, 2H), 7.41-7.35 (m, 2H), 7.20-7.18 (m, 1H), 5.26 (s, 2H); ^{13}C NMR (75 MHz, DMSO-d_6): 172.91, 168.22, 164.27, 160.42 (d, J = 256.49 Hz), 158.53, 141.17, 136.18 (d, J = 8.81 Hz), 134.66, 132.31(d, J = 87.89 Hz), 131.33, 130.12, 128.66, 127.77, 125.89 (d, J = 7.14) Hz), 119.93, 118.21, 117.77 (d, J = 20.66 Hz), 113.60, 112.83 (d, J = 81.22 Hz), 69.25; HRMS (ESI-TOF): calcd for $C_{22}H_{16}FN_3O_4$ $[M + H]^+$ 406.1198, found 406.1199

3-((4-(5-(3-Fluorophenyl)-1,2,4-oxadiazol-3-yl)benzyl)oxy)-N-hydroxybenzamide (12e)

White solid (95 mg, 94.7 %), M.P. 179-180 °C, ^{1}H-NMR (300 MHz, DMSO-d_6): δ 11.26 (s, 1H), 9.11 (s, 1H), 8.12-7.95 (m, 4H), 7.59 (m, 4H), 7.44-7.38 (m, 3H), 7.20 (m, 1H), 5.27 (s, 2H); ^{13}C NMR (75 MHz, DMSO-d_6): δ 174.86, 168.58, 164.26, 162.64 (d, J = 232.93 Hz), 158.53, 141.22, 134.67, 132.53 (d, J = 4.55 Hz), 132.44 (d, J = 3.70 Hz),

130.11, 128.65, 127.76, 125.76 (d, J = 7.58 Hz), 124.73, 120.87 (d, J = 18.66 Hz), 119.91, 118.18, 115.14 (d, J = 24.21 Hz), 113.57, 69.24; HRMS (ESI-TOF): calcd for $C_{22}H_{16}FN_3O_4$ $[M + H]^+$ 406.1198, found 406.1201.

3-((4-(5-Benzyl-1,2,4-oxadiazol-3-yl)benzyl)oxy)-N-hydroxybenzamide (12f)

White solid (93 mg, 92.7 %), M.P. 165-167 °C, ^{1}H-NMR (300 MHz, DMSO-d_6): δ 11.19 (s, 1H), 9.03 (s, 1H), 8.02-8.00 (m, 2H), 7.64-7.61 (m, 2H), 7.39-7.32 (m, 8H), 7.18-7.16 (m, 1H), 5.23 (s, 2H), 4.44 (s, 2H); ^{13}C NMR (75 MHz, DMSO-d_6): δ 179.39, 167.99, 164.26, 158.53, 140.97, 134.67, 134.54, 130.10, 129.56, 129.26, 128.61, 127.83, 127.64, 126.05, 119.92, 118.18, 113.58, 69.23, 32.45; HRMS (ESI-TOF): calcd for $C_{23}H_{19}N_3O_4$ $[M + H]^+$ 402.1448, found 402.1452.

N-hydroxy-3-((4-(5-phenethyl-1,2,4-oxadiazol-3-yl)benzyl)oxy)benzamide (12g)

White solid (95 mg, 94.7 %), M.P. 148-150 °C, ^{1}H-NMR (300 MHz, DMSO-d_6): δ 11.20 (s, 1H), 9.04 (s, 1H), 8.03-8.01 (m, 2H), 7.65-7.62 (m, 2H), 7.40-7.35 (m, 3H), 7.30-7.28 (m, 4H), 7.21-7.16 (m, 2H), 5.24 (s, 2H), 3.33 (m, 2H), 3.13 (t, J = 7.8 Hz, 2H); ^{13}C NMR (75 MHz, DMSO-d_6): δ 180.18, 167.71, 164.25, 158.54, 140.92, 140.14, 134.68, 130.11, 128.90, 128.80, 128.63, 127.60, 126.87, 126.15, 119.91, 118.18, 113.58, 69.24, 32.08, 28.02; HRMS (ESI-TOF): calcd for $C_{24}H_{21}N_3O_4$ $[M + H]^+$ 416.1605, found 416.1609.

3-((4-(5-Ethyl-1,2,4-oxadiazol-3-yl)benzyl)oxy)-N-hydroxy-4-methoxybenzamide (12h)

White solid (89 mg, 88.7 %), M.P. 160-161 °C, ^{1}H-NMR (300 MHz, DMSO-d_6): δ 11.08 (s, 1H), 8.92 (s, 1H), 8.05-8.02 (m, 2H), 7.65-7.62 (m, 2H), 7.47-7.39 (m, 2H), 7.06-7.03 (m, 1H), 5.21 (s, 2H), 3.01 (q, *J* = 6.0 Hz, 2H), 1.34 (t, *J* = 6.0 Hz, 3H); ^{13}C NMR (75 MHz, DMSO-d_6): δ 181.72, 167.73, 164.30, 151.98, 147.58, 140.90, 128.73, 127.56, 126.27, 125.33, 121.02, 112.59, 111.80, 69.93, 56.15, 20.06, 10.91; HRMS (ESI-TOF): calcd for $C_{19}H_{19}N_3O_5$ $[M + H]^+$ 370.1397, found 370.1401.

N-hydroxy-4-methoxy-3-((4-(5-phenyl-1,2,4-oxadiazol-3-yl)benzyl)oxy)benzamide (12i)

White solid (90 mg, 89.7 %), M.P. 184-185 °C, ^{1}H-NMR (300 MHz, DMSO-d_6): δ 11.09 (s, 1H), 8.93 (s, 1H), 8.22-8.19 (m, 2H), 8.15-8.12 (m, 2H), 7.75-7.67 (m, 5H), 7.48-7.39 (m, 2H), 7.07-7.16 (m, 1H), 5.23 (s, 2H), 3.83 (s, 3); ^{13}C NMR (75 MHz, DMSO-d_6): δ 175.90, 168.53, 164.31, 152.01, 147.58, 141.18, 133.84, 130.04, 128.74, 128.39, 127.72, 126.05, 125.35, 123.81, 121.04, 112.66, 111.83, 69.94, 56.17; HRMS (ESI-TOF): calcd for $C_{23}H_{19}N_3O_5$ $[M + H]^+$ 418.1397, found 418.1400.

3-((4-(5-(4-Bromophenyl)-1,2,4-oxadiazol-3-yl)benzyl)oxy)-N-hydroxy-4-methoxybenzamide (12j)

White solid (87 mg, 86.7 %), M.P. 147-148 °C, ^{1}H-NMR (300 MHz, DMSO-d_6): δ 11.10 (s, 1H), 8.93(s, 1H), 8.13 (m, 4H), 7.90 (m, 2H), 7.69 (m, 2H), 7.08-7.05 (m, 1H), 5.24 (s, 2H), 3.84 (s, 3H); ^{13}C NMR (75 MHz, DMSO-d_6): δ 175.19, 168.58, 164.31, 152.01, 147.57, 141.27, 133.17, 130.30, 128.75, 125.89, 125.35, 123.00, 121.06, 112.70,

111.85, 69.95, 56.20; HRMS (ESI-TOF): calcd for $C_{23}H_{18}BrN_3O_5$ $[M + H]^+$ 496.0503, found 496.0495.

Preparation of methyl 3-(cyanomethoxy)-4-methoxybenzoate (13).

To a solution of the substrate **6b** (1.0 g, 5.49 mmol, 1 equiv.) in acetone was added potassium carbonate (2.3 g, 16.48 mmol, 3 equiv.), potassium iodide (91 mg, 0.55 mmol, 0.1 equiv.), and bromoacetonitrile (790 mg, 6.59 mmol, 1.2 equiv.). The mixture was heated to reflux for 4 h. After the reaction was finished, the mixture was filtered and the filtrate was concentrated and purified by chromatography on silica gel to afford the target product (1.1 g, 91.7 %).

General procedure for the preparation of compounds 14a – 14e.

Compounds **13** (200 mg, 1 equiv.) was added to a mixture of hydroxylamine hydrochloride (5 equiv.) and sodium bicarbonate (7 equiv.) in ethanol. The reaction mixture was heated to 80 °C for 40 min. Upon cooling to room temperature, the reaction was filtered and the filtrate evaporated under reduced pressure. After vacuum drying of the solid in a flask, additional reagents carboxylic acid (1 equiv.), 4-dimethylaminopyridine (0.5 equiv.), and 1-ethyl-3-(3-dimethylaminopropyl)carbodiimide hydrochloride (2 equiv.) were added into the flask. The mixture was dissolved by N,N-dimethylformamide (2 mL) and stirred for 12 h at room temperature. Then the reaction was heated to 120 °C for 4 h. After the reaction was finished, the mixture was diluted with water and extracted by

ethyl acetate. The organic phase was washed 3 times by saline and dried over Na_2SO_4. The solution was concentrated and purified by chromatography on silica gel to afford the target products.

Methyl 4-methoxy-3-((5-phenyl-1,2,4-oxadiazol-3-yl)methoxy)benzoate (14a)

White solid (206 mg, 66.9 %), M.P. 133-134 °C, ^{1}H-NMR (300 MHz, $CDCl_3$): δ 8.19-8.16 (m, 2H), 7.77-7.75 (m, 2H), 7.64-7.52 (m, 3H), 6.95-6.92 (m, 1H), 5.34 (s, 2H), 3.94 (s, 3H), 3.89 (s, 3H); ESI-MS m/z: 341.1 $[M + H]^+$.

Methyl 3-((5-(2-fluorophenyl)-1,2,4-oxadiazol-3-yl)methoxy)-4-methoxybenzoate (14b)

White solid (220 mg, 67.8 %), M.P. 122-125 °C, ^{1}H-NMR (300 MHz, $CDCl_3$): δ 8.19-8.14 (m, 1H), 7.77-7.75 (m, 2H), 7.64-7.57 (m, 1H), 7.35-7.25 (m, 2H), 6.95-6.92 (m, 1H), 5.37 (s, 2H), 3.94 (s, 3H), 3.89 (s, 3H); ESI-MS m/z: 381.1 $[M + Na]^+$.

Methyl 3-((5-(3-chlorophenyl)-1,2,4-oxadiazol-3-yl)methoxy)-4-methoxybenzoate (14c)

White solid (206 mg, 61.0 %), M.P. 118-119 °C, ^{1}H-NMR (300 MHz, $CDCl_3$): δ 8.17 (m, 1H), 8.07-8.04 (m, 1H), 7.78-7.75 (m, 2H), 7.60-7.57 (m, 1H), 7.51-7.46 (m, 1H), 6.95-6.92 (m, 1H), 5.33 (s, 2H), 3.94 (s, 3H), 3.89 (s, 3H); ESI-MS m/z: 375.0 $[M + H]^+$.

Methyl 3-((5-(4-chlorophenyl)-1,2,4-oxadiazol-3-yl)methoxy)-4-methoxybenzoate (14d)

White solid (221 mg, 65.3 %), M.P. 134-136 °C, ^{1}H-NMR (300 MHz, $CDCl_3$): δ 8.12-8.09 (m, 2H), 7.77-7.74 (m, 2H), 7.53-7.51 (m, 1H), 6.95-6.92 (m, 1H), 5.33 (s, 2H), 3.94 (s, 3H), 3.89 (s, 3H); ESI-MS m/z: 375.1 $[M + H]^+$.

Methyl 3-((5-(3,4-dimethoxyphenyl)-1,2,4-oxadiazol-3-yl)methoxy)-4-methoxybenzoate (14e)

White solid (229 mg, 63.3 %), M.P. 153-154 °C, ^{1}H-NMR (300 MHz, $CDCl_3$): δ 7.81-7.75 (m, 3H), 7.65-7.64 (m, 1H), 7.00-6.92 (m, 2H), 5.31 (s, 2H), 3.98 (s, 3H), 3.94 (s, 3H), 3.89 (s, 3H); ESI-MS m/z: 401.1 $[M + H]^+$.

General procedure for the preparation of compounds 15a – 15e.

Compounds **14a – 14e** were hydrolyzed to get the corresponding carboxylic acid under a condition of NaOH (10 equiv.) in methanol and H_2O (v: v = 1:1). A mixture of the carboxylic acid (100 mg, 1 equiv.), dimethyl formamide (1 drop) and thionyl chloride (3 equiv.) in anhydrous dichloromethane (10 mL) was heated to reflux for 3 h and concentrated to remove the thionyl chloride and solvent. The concentrate was then re-dissolved by anhydrous tetrahydrofuran (10 mL) and slowly added into a solution of hydroxylamine, which was freshly prepared by dissolving hydroxylammonium chloride (5 equiv.) and NaOH (5 equiv.) into tetrahydrofuran (4 mL) and water (0.5 mL). After the drop add, the mixture was stirred at room

temperature for 5 min, concentrated in vacuum and purified by chromatography on silica gel to afford the title product.

N-hydroxy-4-methoxy-3-((5-phenyl-1,2,4-oxadiazol-3-yl)methoxy)benzamide (15a)

White solid (89 mg, 88.7 %), M.P. 186-188 °C, ^{1}H-NMR (300 MHz, DMSO-d_6): δ 11.06 (s, 1H), 8.93 (s, 1H), 8.15-8.12 (m, 2H), 7.73-7.62 (m, 3H), 7.53 (m, 1H), 7.46-7.43 (m, 1H), 7.08-7.06 (m, 1H), 5.35 (s, 2H), 3.82 (s, 3H); ^{13}C NMR (75 MHz, DMSO-d_6): δ 176.04, 167.77, 164.21, 152.07, 146.91, 133.95, 130.08, 128.36, 125.39, 123.61, 121.93, 113.29, 112.14, 62.07, 56.18; HRMS (ESI-TOF): calcd for $C_{17}H_{15}N_3O_5$ $[M + H]^+$ 342.1084, found 342.1087.

3-((5-(2-Fluorophenyl)-1,2,4-oxadiazol-3-yl)methoxy)-N-hydroxy-4-methoxybenzamide (15b)

White solid (94 mg, 93.7 %), M.P. 166-168 °C, ^{1}H-NMR (300 MHz, DMSO-d_6): δ 11.08 (s, 1H), 8.95 (s, 1H), 8.20-8.15 (m, 1H), 7.83-7.77 (m, 1H), 7.58-7.44 (m, 4H), 7.10-7.07 (m, 1H), 5.38 (s, 2H), 3.83 (s, 3H); ^{13}C NMR (75 MHz, DMSO-d_6): δ 167.51, 164.19, 160.44 (d, J = 250.28 Hz), 152.06, 146.87, 136.30 (d, J = 8.99 Hz), 131.27, 126.03 (d, J = 2.56 Hz), 125.38, 121.95, 117.81 (d, J = 20.21 Hz), 113.27, 112.14, 62.00, 56.18; HRMS (ESI-TOF): calcd for $C_{17}H_{14}FN_3O_5$ $[M + H]^+$ 360.0990, found 360.0996.

3-((5-(3-Chlorophenyl)-1,2,4-oxadiazol-3-yl)methoxy)-N-hydroxy-4-methoxybenzamide (15c)

White solid (86 mg, 85.7 %), M.P. 196-198 °C, ^{1}H-NMR (300 MHz, DMSO-d_6): δ 11.08 (s, 1H), 8.95 (s, 1H), 8.14-8.10 (m, 2H), 7.83-7.81 (m, 1H), 7.72-7.69 (m, 1H), 7.53-7.44 (m, 2H), 7.10-7.07 (m, 1H), 5.37 (s, 2H), 3.83 (s, 3H); ^{13}C NMR (75 MHz, DMSO-d_6): δ 174.84, 167.86, 164.18, 152.03, 146.85, 134.67, 133.74, 132.10, 127.83, 127.10, 125.47, 125.37, 121.93, 113.22, 112.10, 61.97, 56.16; HRMS (ESI-TOF): calcd for $C_{17}H_{14}ClN_3O_5$ $[M + H]^+$ 376.0695, found 376.0695.

3-((5-(4-Chlorophenyl)-1,2,4-oxadiazol-3-yl)methoxy)-N-hydroxy-4-methoxybenzamide (15d)

White solid (91 mg, 90.7 %), M.P. 215-216 °C, ^{1}H-NMR (300 MHz, DMSO-d_6): δ 11.06 (s, 1H), 8.94 (s, 1H), 8.16-8.13 (m, 2H), 7.74-7.71 (m, 2H), 7.53 (m, 1H), 7.47-7.44 (m, 1H), 7.09-7.06 (m, 1H), 5.36 (s, 2H), 3.82 (s, 3H); ^{13}C NMR (75 MHz, DMSO-d_6): δ 175.21, 167.84, 164.16, 152.04, 146.87, 138.81, 130.26, 130.20, 125.37, 122.47, 121.92, 113.23, 112.12, 62.00, 56.17; HRMS (ESI-TOF): calcd for $C_{17}H_{14}ClN_3O_5$ $[M + H]^+$ 376.0695, found 376.0694.

3-((5-(3,4-Dimethoxyphenyl)-1,2,4-oxadiazol-3-yl)methoxy)-N-hydroxy-4-methoxybenzamide (15e)

White solid (92 mg, 91.7 %), M.P. 168-169 °C, ^{1}H-NMR (300 MHz, DMSO-d_6): δ 11.10 (s, 1H), 8.97 (s, 1H), 7.77-7.75 (m, 1H), 7.60 (s, 1H), 7.53 (m, 1H), 7.47-7.44 (m, 1H), 7.10-7.07 (m, 1H), 5.33 (s, 2H), 3.89-3.83 (m, 9H); ^{13}C NMR (75 MHz, DMSO-d_6): δ 176.01, 167.56, 164.20, 153.49, 151.99, 149.55, 146.90, 125.36, 122.32,

121.83, 115.77, 113.15, 112.51, 112.06, 110.62, 62.02, 56.30, 56.16; HRMS (ESI-TOF): calcd for $C_{19}H_{19}N_3O_7$ $[M + H]^+$ 402.1296, found 402.1302.

Preparation of compound methyl 3-hydroxyisoxazole-5-carboxylate (16).

1,8-Diazabicyclo[5.4.0]undec-7-ene (0.5 equiv.) was diluted by methanol and added dropwise to a solution of dimethyl acetylenedicarboxylate (1g, 7.0 mmol, 1 equiv.) and hydroxyurea (1 equiv.) in methanol (15mL) at 0 ℃. After stirring of 1 h on the ice, the reaction mixture was concentrated to about 5 mL and following adjusted to acidic property by 10 % HCl aqueous solution. White solid was deposited and filtered. The product was dried under vacuum. White solid (926 mg, 92.0 %), M.P. 98-99 ℃, ^{1}H-NMR (300 MHz, $CDCl_3$): δ 6.63 (s, 1H), 4.00 (s, 3H).

Preparation of compound methyl 3-(decyloxy)isoxazole-5-carboxylate (17).

A mixture of compound **16** (200 mg, 1.40 mmol, 1 equiv.), 1-bromodecane (340 mg, 1.54 mmol, 1.1 equiv.), potassium carbonate (580 mg, 4.20 mmol, 3 equiv.), and potassium iodide (23 mg, 0.14 mmol, 0.1 equiv.) in acetone was heated to reflux for 6 h. As the reaction was finished, the mixture was cooled to room temperature and filtered. The filtrate was concentrated and purified by chromatography on silica gel to afford the target product. White solid (376 mg, 95.1 %), M.P. 44-45 ℃, ^{1}H-NMR (300 MHz, $CDCl_3$): δ 6.50 (s, 1H), 4.26-4.22 (t, J = 6.60 Hz, 2H), 3.91 (s, 3H), 1.80-1.70 (m, 2H), 1.39-1.36 (m, 2H), 1.30-1.23 (m, 12H), 0.87-0.82 (t, J = 6.09 Hz, 3H); ESI-MS m/z: 284.2 $[M + H]^+$.

Preparation of 3-(decyloxy)-N-hydroxyisoxazole-5-carboxamide (18).

Hydroxylamine hydrochloride (4.7 g, 68.1 mmol, 1 equiv.) was dissolved in methanol (24 mL) under N_2 atmosphere at 80 °C. Following a solution of decarbonate (5.72 g, 68.1 mmol, 1 equiv.) in methanol (14 mL) added. The mixture was stirred at 80 °C for 40 min. The potassium hydroxylamine methanol solution was freshly prepared after filtered of the mixture. To a solution of compound **17** (100 mg, 0.35 mmol) in methanol (2 mL), the potassium hydroxylamine methanol solution (2 mL) was added. The reaction mixture was stirred at room temperature for 10 h under N_2 atmosphere. Then the mixture was adjusted to acidic property and the product was deposited. The product was obtained by filtration and recrystallization by tetrahydrofuran and petroleum ether. White solid (96 mg, 95.7 %), M.P. 153-155 °C, ^{1}H-NMR (300 MHz, DMSO-d_6): δ 11.70 (s, 1H), 9.52 (s, 1H), 6.74 (s, 1H), 4.22 (t, J = 6.0 Hz, 2H), 1.76-1.69 (m, 2H), 1.38-1.27 (m, 14H), 0.88 (t, J = 6.0 Hz, 3H); ^{13}C NMR (75 MHz, DMSO-d_6): δ 171.81, 163.19, 153.86, 97.32, 70.69, 31.76, 29.41, 29.16, 29.12, 28.78, 25.64, 22.56, 14.38; HRMS (ESI-TOF): calcd for $C_{14}H_{24}N_2O_4$ $[M + H]^+$ 285.1809, found 285.1815.

Preparation of methyl 3-((4-bromobenzyl)oxy)isoxazole-5-carboxylate (19).

To a solution of the substrate **16** (1 g, 6.99 mmol, 1 equiv.) in acetone was added potassium carbonate (2.90 g, 21 mmol, 3 equiv.), potassium iodide (116 mg, 0.7 mmol, 0.1 equiv.), and 4-Bromobenzyl bromide (2.1 g, 8.39 mmol, 1.2 equiv.). The mixture

was heated to reflux for 4 h. After the reaction was finished, the mixture was filtered and the filtrate was concentrated and purified by chromatography on silica gel to afford the target product (2.0 g, 92.2 %).

General procedure for the preparation of compounds 20a and 20b.

A mixture of the substrate **19** (200 mg), aromatic boracic acid (1.5 equiv.), and tetrakis(triphenylphosphine)palladium(0) (0.05 equiv.), and cesium carbonate (2 equiv.) in 1,4-dioxane (10 mL) was heated to 100 °C for 4 h under N_2 atmosphere. After the reaction was finished, the mixture was filtered and the solid was washed by dichloromethane. The filtrate was concentrated and purified by chromatography on silica gel to afford the target products.

Methyl 3-([1,1'-biphenyl]-4-ylmethoxy)isoxazole-5-carboxylate (20a)

White solid (149 mg, 75.0 %), M.P. 108-110°C, ^{1}H-NMR (300 MHz, $CDCl_3$): δ 7.64-7.58 (m, 4H), 7.54-7.51 (m, 2H), 7.48-7.53 (m, 2H), 7.39-7.34 (m, 1H), 6.59 (s, 1H), 5.36 (s, 2H), 3.95 (s, 3H); ESI-MS m/z: 310.1 $[M + H]^+$.

Methyl 3-((4'-chloro-[1,1'-biphenyl]-4-yl)methoxy)isoxazole-5-carboxylate (20b)

White solid (179 mg, 81.1 %), M.P. 114-116 °C, ^{1}H-NMR (300 MHz, $CDCl_3$): δ 7.60-7.50 (m, 6H), 7.43-7.40 (m, 2H), 6.58 (s, 1H), 5.36 (s, 2H), 3.95 (s, 3H); ESI-MS m/z: 344.1 $[M + H]^+$.

General procedure for the preparation of compounds 21a and 21b.

Hydroxylamine hydrochloride (4.7 g, 68.1 mmol, 1 equiv.) was dissolved in methanol (24 mL) under N_2 atmosphere at 80 °C. Following a solution of decarbonate (5.72 g, 68.1 mmol, 1 equiv.) in methanol (14 mL) added. The mixture was stirred at 80 °C for 40 min. The potassium hydroxylamine methanol solution was freshly prepared after filtered of the mixture. To a solution of compound **20a** or **20b** (100 mg) in methanol (2 mL), the potassium hydroxylamine methanol solution (2 mL) was added. The reaction mixture was stirred at room temperature for 10 h under N_2 atmosphere. Then the mixture was adjusted to acidic property and the product was deposited. The product was obtained by filtration and recrystallization by tetrahydrofuran and petroleum ether.

3-([1,1'-Biphenyl]-4-ylmethoxy)-N-hydroxyisoxazole-5-carboxamide (21a)

White solid (96 mg, 95.7 %), M.P. 190-192 °C, ^{1}H-NMR (300 MHz, DMSO-d_6): δ 11.73 (s, 1H), 9.54(s, 1H), 7.74-7.59 (m, 6H), 7.53-7.38 (m, 3H), 6.83 (s, 1H), 5.36 (s, 2H); ^{13}C NMR (75 MHz, DMSO-d_6): δ 171.47, 163.40, 153.78, 140.81, 140.12, 135.13, 131.89, 131.02, 129.55, 129.43, 128.10, 127.25, 127.20, 97.55, 71.80; HRMS (ESI-TOF): calcd for $C_{17}H_{14}N_2O_4$ $[M + Na]^+$ 333.0846, found 333.0845.

3-((4'-Chloro-[1,1'-biphenyl]-4-yl)methoxy)-N-hydroxyisoxazole-5-carboxamide (21b)

White solid (94 mg, 93.7 %), M.P. 212-213 °C, ^{1}H-NMR (300 MHz, DMSO-d_6): δ 11.70 (s, 1H), 9.51(s, 1H), 7.73-7.70 (m, 4H), 7.59-7.52 (m, 4H), 6.81 (s, 1H), 5.34 (s,

2H); ^{13}C NMR (75 MHz, DMSO-d_6): δ 171.59, 163.41, 153.86, 139.42, 138.92, 135.54, 133.01, 129.54, 129.37, 128.94, 127.21, 97.57, 71.74; HRMS (ESI-TOF): calcd for $C_{17}H_{13}ClN_2O_4$ $[M + H]^+$ 367.0456, found 367.0457.

Biology

In vitro ASM and NSM inhibition assay

ASM was obtained as follows. The human hepatocellular carcinoma cells (Huh 7) were grown in a medium (DMEM; 10 % Gibco) at 37 °C in a humidified 5.0 % CO_2 incubator. As the cells grown to a confluence of 95 %, they were washed with PBS and lysed in lysis buffer (25 mM Tris-HCl, PH 7.4, 5 mM EDTA). The cells were gathered to an eppendorf tube and broken by Ultrasonic Processor with a strength of 10 %. Cell debris was removed by centrifugation at 300 g for 5 min at 4 °C. The supernatant was transferred to a new eppendorf tube and the concentration of protein was detected by the BCA method.

Recombinant Human ASM (His62 – Pro628, purity >95%) was purchased from Bio-Techne. Quantitative analysis of ASM activity was performed on 400 μg of total cellular protein extract or 20 ng pure ASM protein. NBD–sphingomyelin was purchased from Avanti (AL, USA). NBD-sphingomyelin (1 mg/mL, 4 μL) was suspended in 250 μL of enzyme buffer (100 mM sodium acetate pH 4.7, 1 % Triton X-100, 40 mM $CaCl_2$, 100 μM $ZnCl_2$) and added to the protein extract. Inhibitors were added in various concentrations in DMSO. The total volume of the reaction was

adjusted to 500 μL by addition of water and incubated at 37 °C for 30 min. The reaction was stopped by addition of 800 μL of chloroform / methanol (v/v = 2:1), and phases were separated by centrifugation. After a thin layer chromatography (TLC) of the organic phase, enzymatic activity was determined by measuring the fluorescence intensity of produced NBD-Cers. The results refer to the mean values resulting from three independent experiments.

The in vitro assay for NSM was similar to that of ASM. However, the reaction buffer used for the NSM test is different: 200 mM Tris-HCl buffer (pH 7.4) including 10 mM $MgCl_2$ and 10 mM dithiothreitol.

Cytotoxic assay

Human NIH3T3 cells were maintained in DMEM medium supplemented with 10 % fetal bovine serum under 37 °C and 5 % CO_2. As the cells grown overnight, inhibitor was added into the cell culture. The cells were incubated for another 24 h. Viability of cells was tested using the MTT method.

In vitro cellular uptake.

Human microvascular endothelial hCMEC/D3 cells (purchased from Cell Bank of Chinese Academy of Sciences) were inoculated at the density of 2×10^5 cells/ well in a 24-well cell culture plate. Compound **21b** was added when the cells grew to 80 % (The final concentration was 40 μM, 12.92 μg/mL). Cells treated with serum-free

medium were set as control group. At different time points, the cultured cells were washed twice with ice PBS, and then 100 μL of cell lysate was added to each well. The plate was shaken in ice for 30 min. Cells and lysate were collected, and then centrifuged at 12000 rpm 4 °C for 15 min. Total protein in the lysate was determined by BCA kit (purchased from biyuntian). The content of **21b** in the lysate was determined by HPLC, and the amount of total protein in the cell was determined to calculate the uptake of **21b**. Uptake rate was calculated by the ratio of the concentration of **21b** in lysate to the original dose concentration (12.92 μg/mL).

***In vivo* brain exposure.**

All animal experiments performed in the manuscript were conducted in compliance with institutional guidelines. Nine female SD rats were randomly divided into 3 groups. Compound **21b** was administered to all the rats at 48 mg/Kg. At each time point (0.5 h, 2, h, 4 h), the corresponding rats were deeply anesthetized by CO_2. Then blood samples were collected by heart puncture (0.15 mL), and were placed into anti-coagulant tubes containing EDTA-K2. Following the brain tissue samples were collected immediately. The whole blood samples were centrifuged at 1500 g for 10 min, after which the plasma was separated and the upper plasma samples were collected into the sample tube. The brain tissue samples were all precisely weighed. Then 20 % methanol water was added according to the proportion of weight-volume ratio 1:5 (tissue: homogenizer) for homogenization treatment. Finally, all samples

were quantitatively analyzed by LC-MS/MS (API4000, Agilent ZORBAX XDB-C_{18}, 5 μm, 2.1×50 mm). No hemolysis or clinical abnormalities were found during the whole experiment.

***In vivo* pharmacological studies.**

All animal experiments performed in the manuscript were conducted in compliance with institutional guidelines. The experiments were performed on female SD rats (6-8 weeks, 200 g) purchased from Shanghai SLAC Laboratory Animal Co., Ltd. Reserpine (4 mg/Kg) was used to induce depression by intraperitoneal daily. Compound **21b** was dissolved in DMSO (5 %), Tween 80 (2 %), and glucose (5 %) solution and administered to the rats at 3, 6, and 12 mg/kg by intraperitoneal twice a day for two weeks.

Sugar water preference test: The drinking water was replaced by 10 % sucrose for 48 h. Then fasting and water were deprived for 20 h. Following the rats were give 10 % sucrose and the volume of drinking was calculated.

Open-field test: A 100 cm×100 cm box was divided into 25 equal squares with surrounding with walls about 42 cm high. The tests were performed at 7:30～12:00. A rat was placed in the central square. The total time in center, times passing the grid, frequency of upright, and frequency of grooming in 5 minutes were recorded.

Relative ASM activity assay

Cerebral cortex and hippocampus were separated from half of the brain. Total protein was extracted and quantified by the BCA method. Quantitative analysis of ASM activity was performed on 300 μg of total protein and 4 μg NBD-sphingomyelin. The reaction was same as above. The activity of the normal control was regarded as 100 %. The relative activity was calculated by fluorescence intensity of produced NBD-Cers on TLC.

Neurogenesis test

Rats were injected with 5-ethynyl-2'-deoxyuridine (EDU) at 8 mg/kg 2-times 1 day. Then rats were sacrificed 96 hours later and the brains were shock frozen and sectioned. Sections were washed with 2 mg/mL glycine and PBS. The sections were stained with 1X Click-iT staining solution for 30 min and washed with 0.5 % TritonX-100. Then the sections were treated with 100 μL 1X Hoechst 33342 for 30 min, washed with PBS, and mounted for fluorescence microscopy.

Ancillary Information

Supporting Information.

Data for the original activity data and spectra of the title compounds.

Molecular formula strings.

Author Information

Corresponding authors

*Jinxin Wang: Phone: +86 13770600394, Email: jinxinwangcpu@126.com

*Jibin Dong: Phone +86 13621869727, Email: jbdong@shmu.edu.cn

Author contributions

These authors contributed equally to this work.

Notes

The authors declare no competing financial interest.

Acknowledgments

This work was supported financially by the Double First-Class initiative new drug development and construction project of China Pharmaceutical University (CPU2018PZQ07), by the scientific research foundation for talent introduction of Hebei university (801260201283), by the Natural Science Foundation of Jiangsu Province (BK20191318). We also thank the Super-Computer-Center of Hebei university for computational supports.

Abbreviations Used

ASM, acid sphingomyelinase; SM, sphingomyelin; Cers, ceramide; ZBG, zinc binding groups; NSM, neutral sphingomyelinase; MDD, major depression disorder.

References

1. Belmaker, R. H.; Agam, G. Mechanisms of disease: major depressive disorder. *New*

Engl J Med **2008,** 358, 55-68.

2. David, D. J.; Gourion, D. Antidepressant and tolerance: determinants and management of major side effects. *Encephale-Revue De Psychiatrie Clinique Biologique Et Therapeutique* **2016,** 42, 553-561.

3. Mrazek, D. A.; Hornberger, J. C.; Altar, C. A.; Degtiar, I. A review of the clinical, economic, and societal burden of treatment-resistant depression: 1996–2013. *Psychiatr Serv* **2014,** 65, 977-987.

4. Lang, U. E.; Borgwardt, S. Molecular mechanisms of depression: perspectives on new treatment strategies. *Cell Physiol Biochem* **2013,** 31, 761-777.

5. Santarelli, L.; Saxe, M.; Gross, C.; Surget, A.; Battaglia, F.; Dulawa, S.; Weisstaub, N.; Lee, J.; Duman, R.; Arancio, O.; Belzung, C.; Hen, R. Requirement of hippocampal neurogenesis for the behavioral effects of antidepressants. *Science* **2003,** 301, 805-809.

6. Egeland, M.; Guinaudie, C.; Du Preez, A.; Musaelyan, K.; Zunszain, P. A.; Fernandes, C.; Pariante, C. M.; Thuret, S. Depletion of adult neurogenesis using the chemotherapy drug temozolomide in mice induces behavioural and biological changes relevant to depression. *Transl Psychiatry* **2017,** 7, e1101.

7. Mahar, I.; Bambico, F. R.; Mechawar, N.; Nobrega, J. N. Stress, serotonin, and hippocampal neurogenesis in relation to depression and antidepressant effects. *Neurosci Biobehav Rev* **2014,** 38, 173-192.

8. Gulbins, E.; Walter, S.; Becker, K. A.; Halmer, R.; Liu, Y.; Reichel, M.; Edwards,

M. J.; Muller, C. P.; Fassbender, K.; Kornhuber, J. A central role for the acid sphingomyelinase/ceramide system in neurogenesis and major depression. *J Neurochem* **2015,** 134, 183-192.

9. Jernigan, P. L.; Hoehn, R. S.; Grassme, H.; Edwards, M. J.; Muller, C. P.; Kornhuber, J.; Gulbins, E. Sphingolipids in major depression. *Neurosignals* **2015,** 23, 49-58.

10. Ong, W. Y.; Herr, D. R.; Farooqui, T.; Ling, E. A.; Farooqui, A. A. Role of sphingomyelinases in neurological disorders. *Expert Opin Ther. Targets* **2015,** 19, 1725-1742.

11. Stancevic, B.; Kolesnick, R. Ceramide-rich platforms in transmembrane signaling. *FEBS Lett* **2010,** 584, 1728-1740.

12. Huwiler, A.; Fabbro, D.; Pfeilschifter, J. Selective ceramide binding to protein kinase C-α and -δ isoenzymes in renal mesangial cells. *Biochemistry* **1998,** 37, 14556-14562.

13. Heinrich, M.; Neumeyer, J.; Jakob, M.; Hallas, C.; Tchikov, V.; Winoto-Morbach, S.; Wickel, M.; Schneider-Brachert, W.; Trauzold, A.; Hethke, A.; Schutze, S. Cathepsin D links TNF-induced acid sphingomyelinase to Bid-mediated caspase-9 and -3 activation. *Cell Death Differ* **2004,** 11, 550-563.

14. Garcia-Ruiz, C.; Morales, A.; Fernandez-Checa, J. C. Glycosphingolipids and cell death: one aim, many ways. *Apoptosis* **2015,** 20, 607-620.

15. Morad, S. A.; Cabot, M. C. Ceramide-orchestrated signalling in cancer cells. *Nat Rev*

Cancer **2013,** 13, 51-65.

16. Niaudet, C.; Bonnaud, S.; Guillonneau, M.; Gouard, S.; Gaugler, M. H.; Dutoit, S.; Ripoche, N.; Dubois, N.; Trichet, V.; Corre, I.; Paris, F. Plasma membrane reorganization links acid sphingomyelinase/ceramide to p38 MAPK pathways in endothelial cells apoptosis. *Cell Signal* **2017,** 33, 10-21.

17. Kornhuber, J.; Medlin, A.; Bleich, S.; Jendrossek, V.; Henkel, A. W.; Wiltfang, J.; Gulbins, E. High activity of acid sphingomyelinase in major depression. *J Neural Transm (Vienna)* **2005,** 112, 1583-1590.

18. Gracia-Garcia, P.; Rao, V.; Haughey, N. J.; Bandaru, V. V.; Smith, G.; Rosenberg, P. B.; Lobo, A.; Lyketsos, C. G.; Mielke, M. M. Elevated plasma ceramides in depression. *J Neuropsychiatry Clin Neurosci* **2011,** 23, 215-218.

19. Rhein, C.; Reichel, M.; Kramer, M.; Rotter, A.; Lenz, B.; Muhle, C.; Gulbins, E.; Kornhuber, J. Alternative splicing of SMPD1 coding for acid sphingomyelinase in major depression. *J. Affect. Disord.* **2017,** 209, 10-15.

20. Kornhuber, J.; Tripal, P.; Reichel, M.; Terfloth, L.; Bleich, S.; Wiltfang, J.; Gulbins, E. Identification of new functional inhibitors of acid sphingomyelinase using a structure-property-activity relation model. *J Med Chem* **2008,** 51, 219-237.

21. Kornhuber, J.; Tripal, P.; Gulbins, E.; Muehlbacher, M. Functional inhibitors of acid sphingomyelinase (FIASMAs). *Handb Exp Pharmacol* **2013**, 169-186.

22. Gulbins, E.; Palmada, M.; Reichel, M.; Luth, A.; Bohmer, C.; Amato, D.; Muller, C.

P.; Tischbirek, C. H.; Groemer, T. W.; Tabatabai, G.; Becker, K. A.; Tripal, P.; Staedtler, S.; Ackermann, T. F.; van Brederode, J.; Alzheimer, C.; Weller, M.; Lang, U. E.; Kleuser, B.; Grassme, H.; Kornhuber, J. Acid sphingomyelinase-ceramide system mediates effects of antidepressant drugs. *Nat Med* **2013,** 19, 934-938.

23. Grassme, H.; Jernigan, P. L.; Hoehn, R. S.; Wilker, B.; Soddemann, M.; Edwards, M. J.; Muller, C. P.; Kornhuber, J.; Gulbins, E. Inhibition of acid sphingomyelinase by antidepressants counteracts stress-induced activation of P38-kinase in major depression. *Neurosignals* **2015,** 23, 84-92.

24. Muller, C. P.; Kalinichenko, L. S.; Tiesel, J.; Witt, M.; Stockl, T.; Sprenger, E.; Fuchser, J.; Beckmann, J.; Praetner, M.; Huber, S. E.; Amato, D.; Muhle, C.; Buttner, C.; Ekici, A. B.; Smaga, I.; Pomierny-Chamiolo, L.; Pomierny, B.; Filip, M.; Eulenburg, V.; Gulbins, E.; Lourdusamy, A.; Reichel, M.; Kornhuber, J. Paradoxical antidepressant effects of alcohol are related to acid sphingomyelinase and its control of sphingolipid homeostasis. *Acta Neuropathol* **2017,** 133, 463-483.

25. Arenz, C. Small molecule inhibitors of acid sphingomyelinase. *Cell Physiol Biochem* **2010,** 26, 1-8.

26. Sakata, A.; Yasuda, K.; Ochiai, T.; Shimeno, H.; Hikishima, S.; Yokomatsu, T.; Shibuya, S.; Soeda, S. Inhibition of lipopolysaccharide-induced release of interleukin-8 from intestinal epithelial cells by SMA, a novel inhibitor of sphingomyelinase and its therapeutic effect on dextran sulphate sodium-induced colitis in mice. *Cell Immunol*

2007, 245, 24-31.

27. Roth, A. G.; Drescher, D.; Yang, Y.; Redmer, S.; Uhlig, S.; Arenz, C. Potent and selective inhibition of acid sphingomyelinase by bisphosphonates. *Angew Chem Int Ed Engl* **2009,** 48, 7560-7563.

28. Roth, A. G.; Redmer, S.; Arenz, C. Development of carbohydrate-derived inhibitors of acid sphingomyelinase. *Bioorg Med Chem* **2010,** 18, 939-944.

29. Roth, A. G.; Redmer, S.; Arenz, C. Potent inhibition of acid sphingomyelinase by phosphoinositide analogues. *ChemBioChem* **2009,** 10, 2367-2374.

30. Wetzel, S.; Wilk, W.; Chammaa, S.; Sperl, B.; Roth, A. G.; Yektaoglu, A.; Renner, S.; Berg, T.; Arenz, C.; Giannis, A.; Oprea, T. I.; Rauh, D.; Kaiser, M.; Waldmann, H. A scaffold-tree-merging strategy for prospective bioactivity annotation of gamma-pyrones. *Angew. Chem Int Ed Engl* **2010,** 49, 3666-3670.

31. Hamada, M.; Iikubo, K.; Ishikawa, Y.; Ikeda, A.; Umezawa, K.; Nishiyama, S. Biological activities of alpha-mangostin derivatives against acidic sphingomyelinase. *Bioorg. Med Chem Lett* **2003,** 13, 3151-3153.

32. Yang, K.; Gao, B.; Ming, X.; Huang, Z.; Wang, M.; Dong, J.; Wang, J. Synthesis and evaluation of xanthone derivatives as acid sphingomyelinase inhibitors: potential treatment for UV-induced skin damage. *Future Med Chem* **2017,** 9, 1887-1898.

33. Yang, K.; Nong, K.; Gu, Q.; Dong, J.; Wang, J. Discovery of N-hydroxy-3-alkoxybenzamides as direct acid sphingomyelinase inhibitors using a

ligand-based pharmacophore model. *Eur J Med Chem* **2018,** 151, 389-400.

34. Gorelik, A.; Illes, K.; Heinz, L. X.; Superti-Furga, G.; Nagar, B. Crystal structure of mammalian acid sphingomyelinase. *Nat Commun* **2016,** 7, 12196.

35. Xiong, Z. J.; Huang, J.; Poda, G.; Pomes, R.; Prive, G. G. Structure of human acid sphingomyelinase reveals the role of the saposin domain in activating substrate hydrolysis. *J Mol Biol* **2016,** 428, 3026-3042.

36. Zhou, Y. F.; Metcalf, M. C.; Garman, S. C.; Edmunds, T.; Qiu, H.; Wei, R. R. Human acid sphingomyelinase structures provide insight to molecular basis of Niemann-Pick disease. *Nat Commun* **2016,** 7, 13082.

37. Salic, A.; Mitchison, T. J. A chemical method for fast and sensitive detection of DNA synthesis in vivo. *Proc Natl Acad Sci U S A* **2008,** 105, 2415-2420.

Table of Contents Graphic

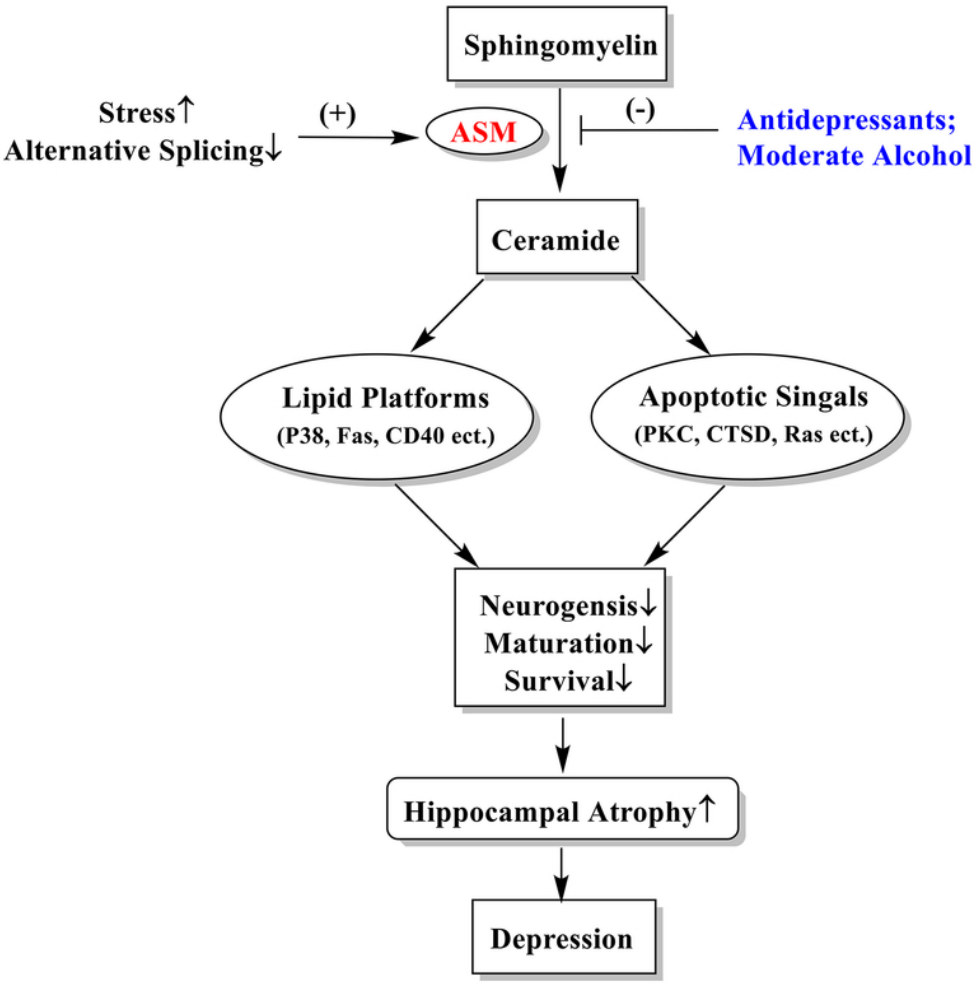

Figure 1 Supposed mechanism of acid sphingomyelinase in the development of depression. ASM, acid sphingomyelinase

33x33mm (600 x 600 DPI)

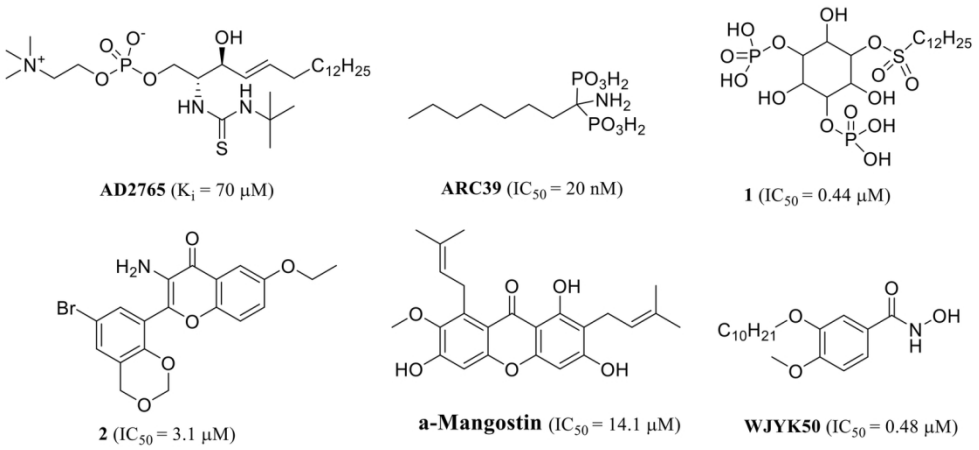

Figure 2 Representative structures of acid sphingomyelinase inhibitors.

69x32mm (600 x 600 DPI)

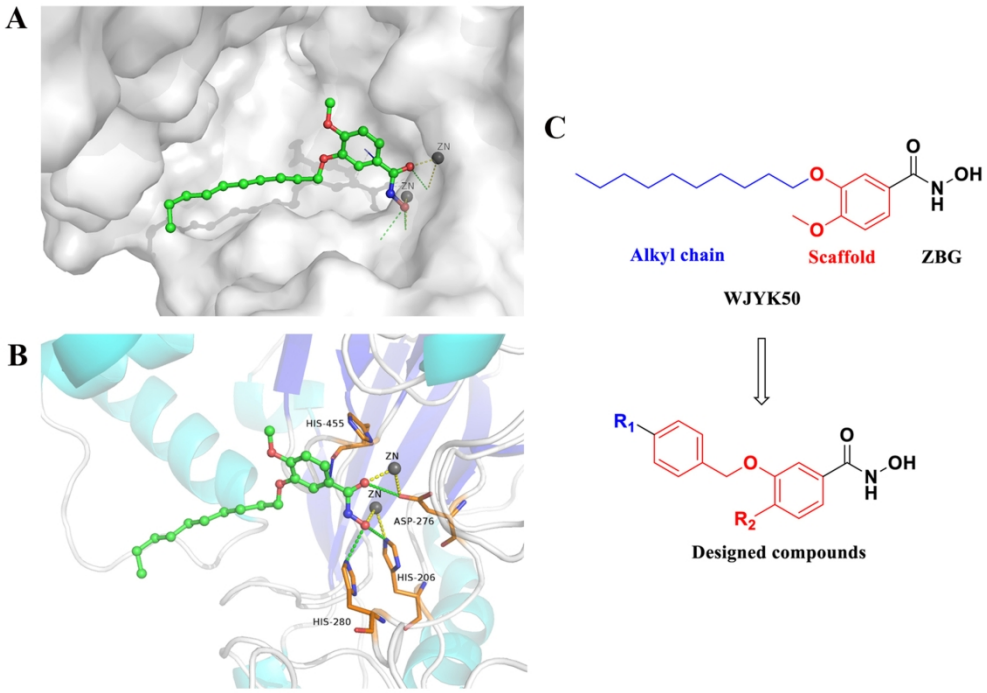

Figure 3 Docking pose of WJYK50 in acid sphingomyelinase and optimizing strategy. Hydrogen bonds are shown as green lines and metal contacts in yellow.

177x124mm (300 x 300 DPI)

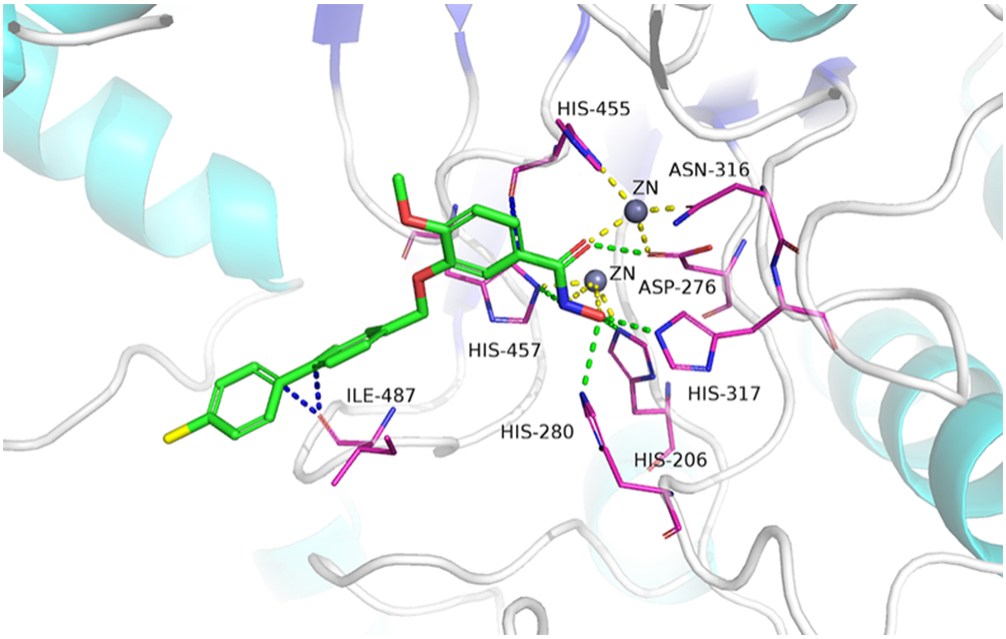

Figure 4 Docking poses of 9f identified in acid sphingomyelinase. Hydrogen bonds are shown as green lines, metal contacts in yellow, and Pi contacts in blue.

84x53mm (300 x 300 DPI)

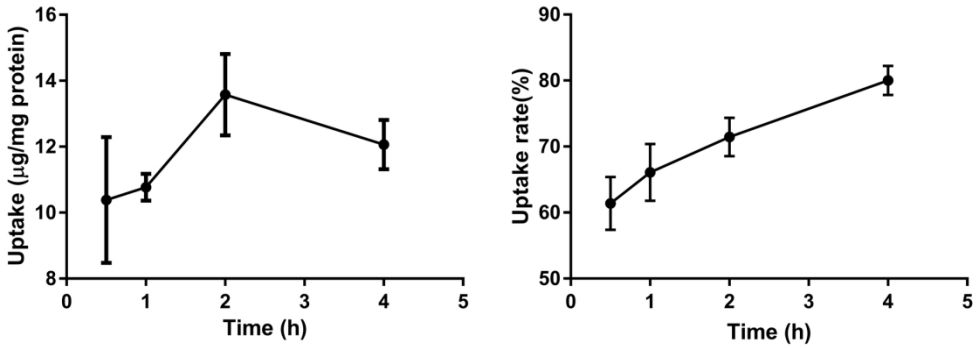

Figure 5 Cellular uptake of 21b in hCMEC/D3 cells. Values are expressed as mean ± SD from 3 independent experiments.

84x31mm (600 x 600 DPI)

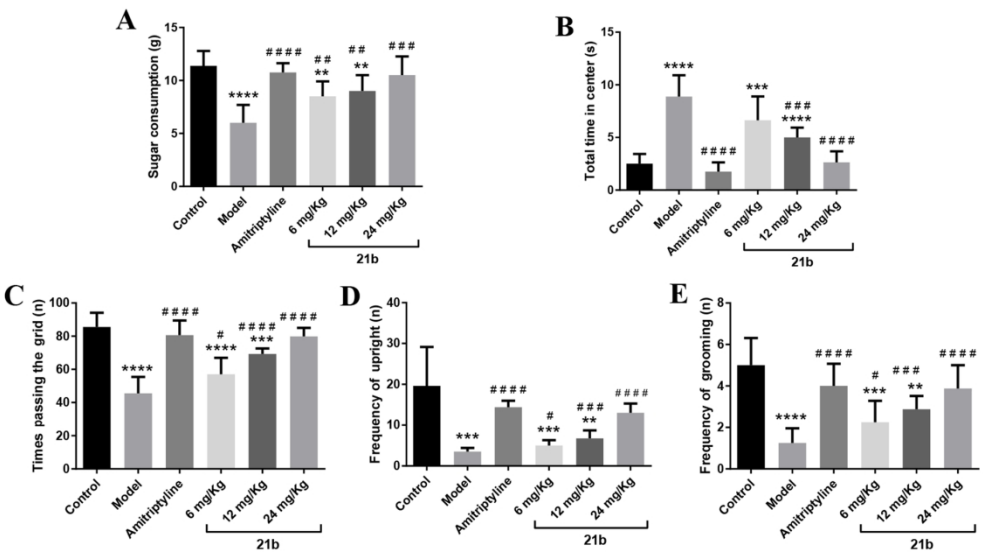

Figure 6 Anti-depressant effect of compound 21b. Amitriptyline was used as 12 mg/Kg. A, sugar water preference test. B-D, open-field test. Values are expressed as mean ± SD from 8 independent experiments. *, P value compared to control group (**p<0.01, ***p<0.001, ****p<0.0001). #, P value compared the model group (# p<0.05, # # p<0.01, # # # p<0.001, # # # # p<0.0001).

172x96mm (300 x 300 DPI)

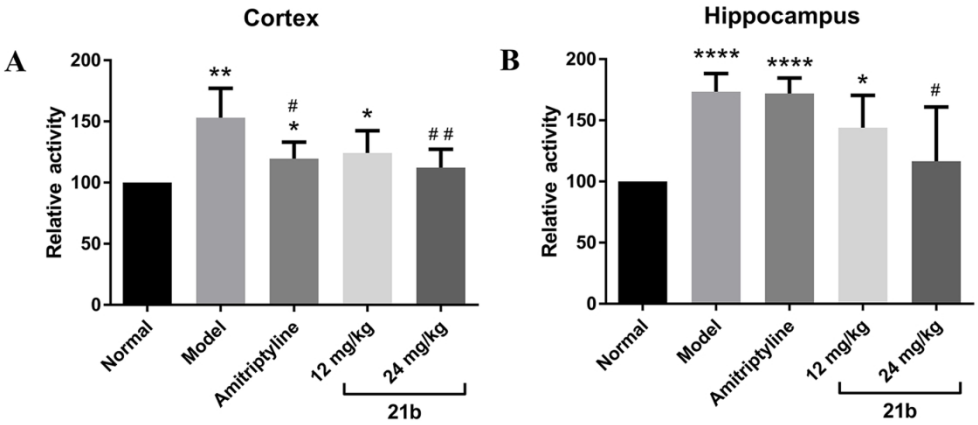

Figure 7 Relative acid sphingomyelinase activity in cerebral cortex and hippocampus. Amitriptyline was used as 12 mg/Kg. The activity of the normal group was regarded as 100 %, and the Y-axis reflected the relative percentage of each group to the normal group. Values are expressed as mean ± SD from 5 independent experiments. *, P value compared to control group (*p<0.05, **p<0.01, ****p<0.0001). #, P value compared the model group (# p<0.05, # # p<0.01).

84x37mm (600 x 600 DPI)

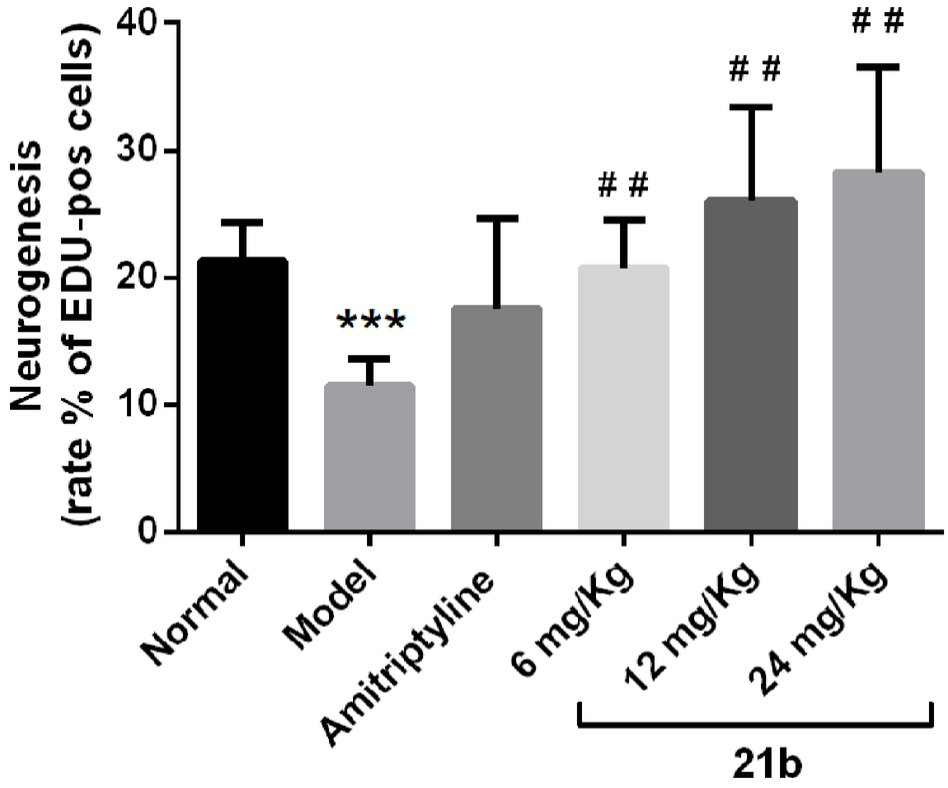

Figure 8 Neurogenesis in hippocampus. The dose of amitriptyline was 12 mg/Kg. Values are expressed as mean ± SD from 5 independent experiments, ***p<0.005 compared to control group, # # p<0.01 compared the model group.

84x73mm (300 x 300 DPI)